CALIFORNIA STATE UNIVERSITY, NORTHRIDGE

QUATERNARY STRATIGRAPHY AND GEOLOGIC EVOLUTION OF OJAI AND UPPER OJAI VALLEYS, WESTERN TRANSVERSE RANGES, CALIFORNIA

A thesis submitted in partial fulfillment of the requirements
For the degree of Master of Science in Geology

By

Hannah Lynne McKay

December 2011

Signature Page

The thesis of Hannah Lynne McKay is approved:

Elena A. Miranda, Ph.D.	Date
J. Doug Yule, Ph.D.	Date
Richard V. Heermance, Ph.D., chair	Date

California State University, Northridge

Dedication

This project is dedicated to my parents who have always instilled the importance of education, have never failed to give me unconditional love and support, and for teaching me that even the largest task can be accomplished if it is done one step at a time.

Acknowledgements

I would like to acknowledge Dr. Richard Heermance, committee chair, for his enthusiastic advice, guidance, and financial assistance. I attribute the level of my Masters degree to his effort and support. One simply could not wish for a better advisor. I also thank the members of my graduate committee, Dr. Elena Miranda and Dr. Doug Yule for their guidance and suggestions.

Additionally, I thank the Southern California Earthquake Center (SCEC) for grant 09004, awarded to Dr. Heermance, and the California State University Northridge Geology Department for numerous scholarships and financial assistance.

I recognize Scott Minor and Jordan Kear whom provided insight and guidance in the Ojai area throughout the preliminary stages of fieldwork. In addition, fieldwork could not be completed without the approval of Sandra Moore, Mary Bergen, Ojai Valley School, and Villanova School for access to private property.

I thank Dr. Bodo Bookhagen and Burch Fisher for access and assistance in the University of California Santa Barbara cosmogenic lab. Also, I thank Paul McBurnett for processing radiocarbon samples.

Table of Contents

List of Figures

List of Tables

Abstract

QUATERNARY STRATIGRAPHY AND GEOLOGIC EVOLUTION
OF OJAI AND UPPER OJAI VALLEYS,
WESTERN TRANSVERSE RANGES, CALIFORNIA

By

Hannah Lynne McKay

Master of Science in Geology

Ojai and Upper Ojai valleys are intramontane basins in the western Transverse Ranges filled with strata that have recorded the uplift of surrounding ranges, evolution of the drainage system, and landscape development since mid Quaternary time. A combination of careful mapping and stratigraphic description of exhumed strata combined with subsurface water- and oil-well data document the late-Quaternary provenance changes, depositional settings, and geometry of the basin fill.

New measured sections, clast counts, and mapping suggest that initial deposition consisted of fluvial gravels in a braided river system that flowed to the west with material derived from the ranges in the northeast. The deposits are preserved in two depocenters, 240 m and 500 m deep, below the modern Ojai and Upper Ojai valleys, respectively. The locations of depocenters are structurally controlled so the minimum ages of the depocenters are based on the age of the basin-bounding faults, which are calculated from slip rates published by previous workers and the vertical separation of the base of the basin fill on either side of the fault. In Upper Ojai Valley the depocenter formed due to uplift of Sulphur Mountain along the Lion, Sisar, and Big Canyon faults more than 415 ± 85 ka. The depocenter in Ojai Valley formed behind Black Mountain, which uplifted along the Arroyo Parida-Santa Ana fault more than 265 ± 15 ka.

Toward the end of basin filling, Sulphur Mountain began contributing clasts to the basin fill. Soon after, the emplacement of a landslide dam in the western end of Upper Ojai Valley allowed for the formation of a lake in Upper Ojai Valley from greater than 46 to ~ 15 ka, as evident by radiocarbon dating of organic material. The landslide dam, as well as tectonic tilting, caused a change in base level that led to incised meanders in Lion Canyon and reversal of flow of Sisar Creek to the east. Later change in base level, perhaps due to the uplift of the Oak View area to the south of the Arroyo Parida-Santa Ana fault, also caused the incision of San Antonio Creek and the Ventura River.

This work implies that the basin fill in Ojai and Upper Ojai valleys are a separate entity from the rest of the Ventura Basin stratigraphy. Also, the fill is neither Holocene terrace deposits nor middle Quaternary Saugus Formation equivalent in which it has previously been interpreted. The rapid deposition, deformation, and preservation of these deposits are important aspects for potential oil and groundwater reservoirs as well as convergence rates that affect the seismic hazard for the region.

1. INTRODUCTION

Studies of fault-bounded intramontane basins have demonstrated that the sedimentary units contained within are important recorders of uplift, erosion, drainage evolution, and syntectonic deposition within actively growing topography (*e.g.* Ori & Friend, 1984; Decelles & Giles, 1996; Horton *et al.*, 2002; Kumar *et al.*, 2007; Heermance *et al.*, 2007). Additionally, intramontane basin sediments rest on orogenically deformed and erosionally truncated basement and the upper basin sediments are commonly dissected by modern fluvial systems and active faults. Thus, intramontane basins provide an intermediate scale (10^4-10^6 years) link between long-term (10^6-10^7 years) plate tectonic scale deformation and short-term (10^1-10^3 years) climatic and tectonic processes (*e.g.* Brookfield, 1980; Burbank and Johnson, 1983; and Searle *et al.*, 1990; Donnellan *et al.*, 1993; Allen *et al.*, 2004).

The Ojai and Upper Ojai valleys are actively deforming intramontane basins within the western Transverse Ranges (wTR) of southern California (figure 1). Ojai and Upper Ojai valleys are bounded by actively growing mountain ranges and are filled with Quaternary conglomeratic deposits. Previous workers have interpreted the conglomerates in the Ojai valleys as Saugus Formation (e.g. Rockwell et al., 1988; Yeats et al., 1988;

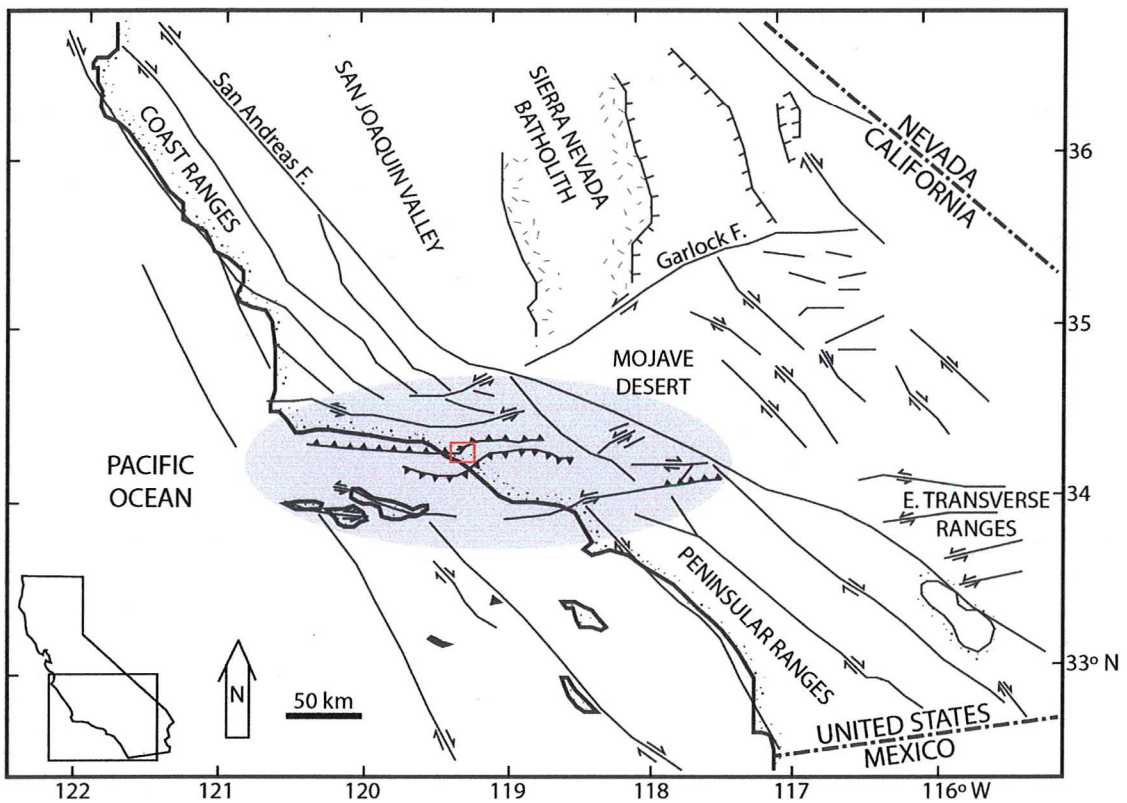

Figure 1. Map of southern California showing locations of the wTR province (shaded), significant geographic features, and major faults (modified from Jackson and Molnar, 1990). The red box denotes the approximate location of Ojai and Upper Ojai valleys within the wTR region.

Huftile, 1991; Huftile and Yeats, 1995) or terrace deposits (Rockwell *et al.*, 1984) that are as little as 200 years old. Hence, the age, lithology, and origin of the basin fill in Ojai and Upper Ojai valleys are undefined. Additionally, the uplift histories of the surrounding ranges are poorly understood.

The lithology and geochronology of the Saugus Formation throughout the wTR varies greatly. Near the city of Ventura (figure 2), the marine portion of the Saugus Formation has been dated between 0.63 and 0.2 Ma based on amino-acid racemization on

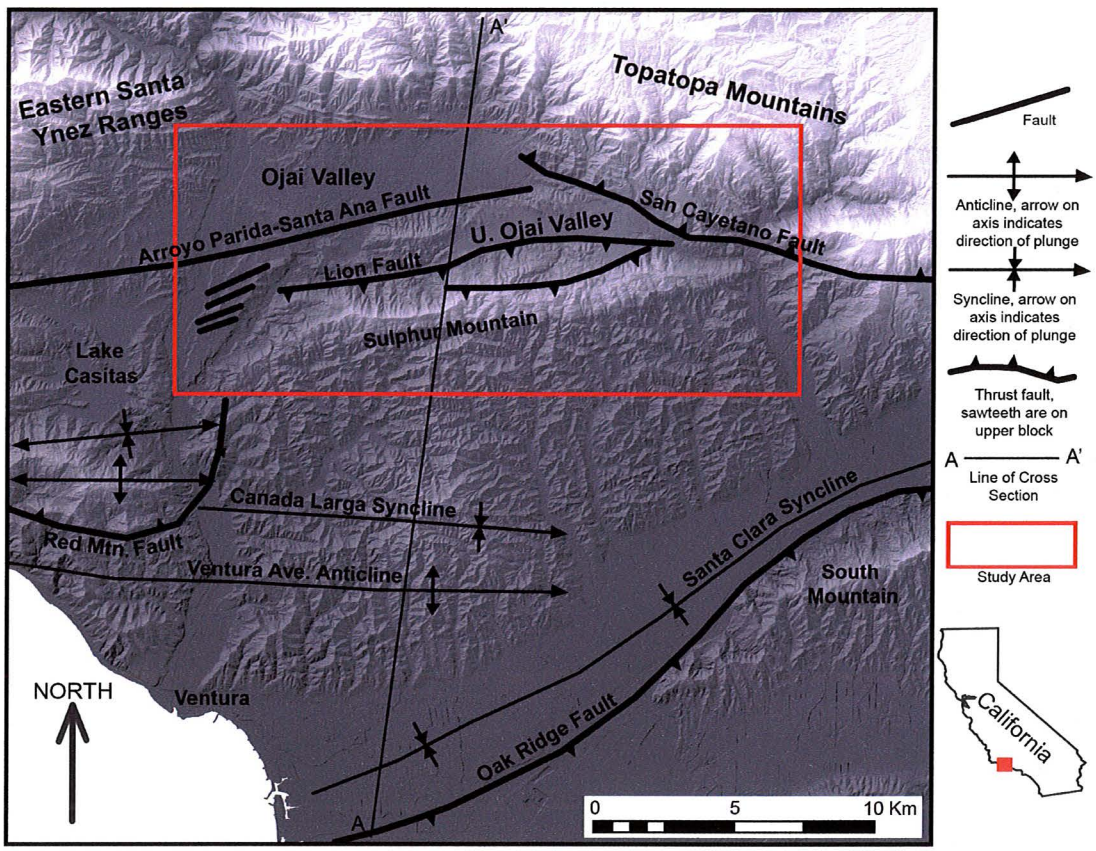

Figure 2. Digital elevation model of the wTR province with approximate locations of major geologic structures. The red box represents the area of interest for this project and cross section A-A' is figure 3a.

bivalve shells (Lajoie *et al.*, 1982) and tephrochronology (Sarna-Wojcicki *et al.*, 1984). The minimum age may be inaccurate due to models used in the amino-acid stereochemistry (Wehmiller *et al.,* 1992). At least 40 km to the east of Ventura, the minimum age of the Saugus Formation is 500 ka, which is based on magnetostratigraphy and constant rates of deposition above and below the Bruhnes-Matuyama boundary (Levi & Yeats, 1993). Therefore, correlation of the conglomerates in the Ojai valleys with the Saugus Formation does not elucidate the age of the basin fill in the Ojai valleys.

Furthermore, Quaternary rates of convergence across the wTR are based on the age and deformation of the Saugus Formation, which is the youngest deformed formation in the region (figure 3). These calculated rates are as fast as 28 mm/year, (Huftile & Yeats, 1995) but imply that the Saugus Formation originally covered and was

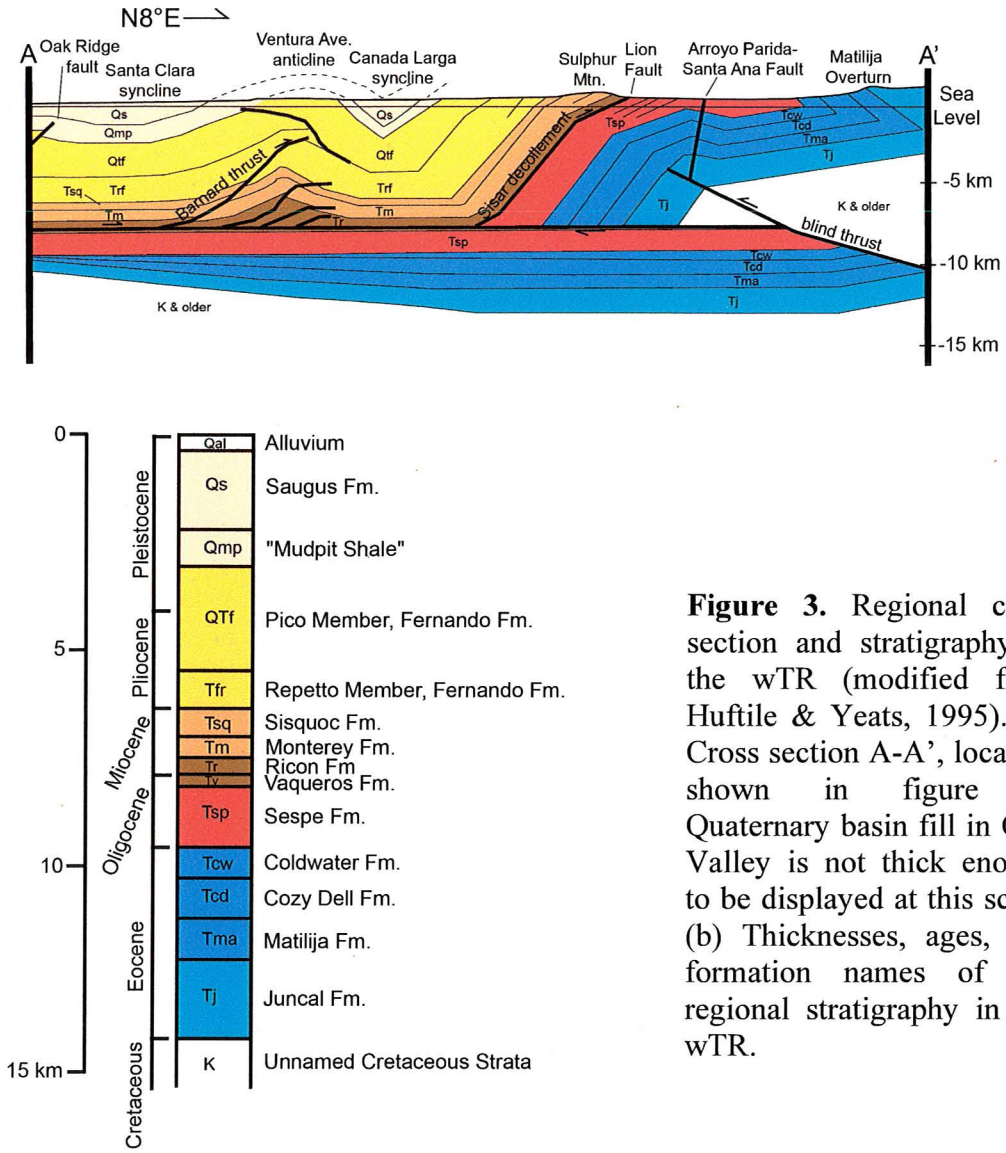

Figure 3. Regional cross section and stratigraphy of the wTR (modified from Huftile & Yeats, 1995). (a) Cross section A-A', location shown in figure 2. Quaternary basin fill in Ojai Valley is not thick enough to be displayed at this scale. (b) Thicknesses, ages, and formation names of the regional stratigraphy in the wTR.

subsequently deformed by Sulphur Mountain, which bounds the Ojai valleys to the south. No direct correlation has been made between the conglomerates in the Ojai valleys and the Saugus Formation, so the calculated Quaternary convergence rates cannot be used to calculate uplift rates of the ranges surrounding the Ojai valleys.

The purpose of this thesis is to elucidate the late Quaternary formation and filling of Ojai and Upper Ojai valleys by studying the basin fill. Luckily, the Quaternary basin fill in the Ojai valleys is exposed due to uplift on the Arroyo Parida-Santa Ana and Lion faults and incision by modern drainages. These exposures, combined with subsurface well data, allow for a sedimentologic, stratigraphic, and geochronologic study of the basin fill. The relationship between the basin fill and the underlying bedrock and active faults is observed to interpret the processes that led to the formation of the intramontane basins. The sedimentology and lithology is observed to interpret the depositional processes and source of the material that filled the basins. Cosmogenic and radiocarbon

geochronologic methods are used to predict the timing of these processes. Lastly, the relationship between the basin fill, active faults, fluvial terraces, and actively incising drainages are used to interpret the Pleistocene landscape evolution in the area.

2. GEOLOGIC BACKGROUND

The wTR have a complex geologic history due to the evolution of the tectonic plate boundary along the western margin of North America. Throughout the Mesozoic and into the Oligocene the western margin of the North American plate was a subduction zone (Atwater, 1998) and the wTR comprised a roughly north-south striking forarc basin called the Ventura Basin (Crowell, 1987). Transition from a subduction zone to the modern San Andreas transform boundary began between 28 and 17 Ma when the East Pacific Rise began subducting below North America (Atwater, 1998). Paleomagnetic data provides evidence for 90-110° of clockwise rotation of the wTR since the early Miocene (Hornafius *et al.*, 1986). Shortening and uplift of the wTR initiated approximately 5 Ma due to reorganization of the plate boundary (Atwater, 1998).

Today, the wTR are an east-west striking deformation belt from 34-35° north that extends from the Santa Barbara channel to the Mojave section of the San Andreas fault (figure 1). Most active faults are roughly east-west striking thrust faults, some with a large left-lateral component that commonly cut folds of similar orientation (Huftile & Yeats, 1996; figures 2 & 3). Due to the preexisting structures and rotation of the wTR, much of the shortening is accommodated on reverse faults that were originally Miocene normal faults and within basins that were formerly north- or northwest-trending extensional features (Luyendyk *et al.*, 1985; Crouch & Suppe, 1993).

Much of the convergence is accommodated in the wTR by thin-skinned thrusting above the Rincon and Sisar decollements (Yeats *et al.*, 1988; figure 3). Major structures, such as the Oak Ridge, San Cayetano, and Santa Susana faults, divide the province into 100-200 km long and 10-30 km wide blocks (Jackson & Molnar, 1990) that have been undergoing clockwise rotation for greater than 15 Ma, since formation of the San Andreas fault began (Atwater, 1998). In addition to fault block models, focal mechanisms of historical earthquakes show that these events accommodate the transpressional regime that is actively uplifting and deforming the region (Hauksson *et al.*, 1995) and geodetic data suggests that the blocks are still rotating at a rate of several degrees per million years (Jackson & Molnar, 1990).

Ojai & Upper Ojai valleys

Ojai and Upper Ojai valleys are intramontane basins located within the wTR. Ojai Valley has an area of ~45 km^2, an elevation of 180-360 m and is approximately 20 km north of the city of Ventura. Upper Ojai Valley is just to the southeast at a slightly higher elevation of 390-420 m. The valleys are situated between the 2,050 m high Topatopa and eastern Santa Ynez Ranges to the north, the 880 m Sulphur Mountain to the south, the Ventura River to the west, Santa Paula Creek to the east, and are separated by Black Mountain (figure 4).

The modern drainage system in the study area is dominated by the Ventura River, which flows to the south along the western edge of Ojai Valley (figure 4). San Antonio Creek flows westward through Ojai Valley and has a drainage basin area of 130 km^2 before it joins with the Ventura River (figure 4). Lion Creek flows parallel to San Antonio Creek, drains most of Upper Ojai Valley, and has a drainage basin area of about 30 km^2 (figure 4). Lion Creek flows through Lion Canyon before joining San Antonio Creek and

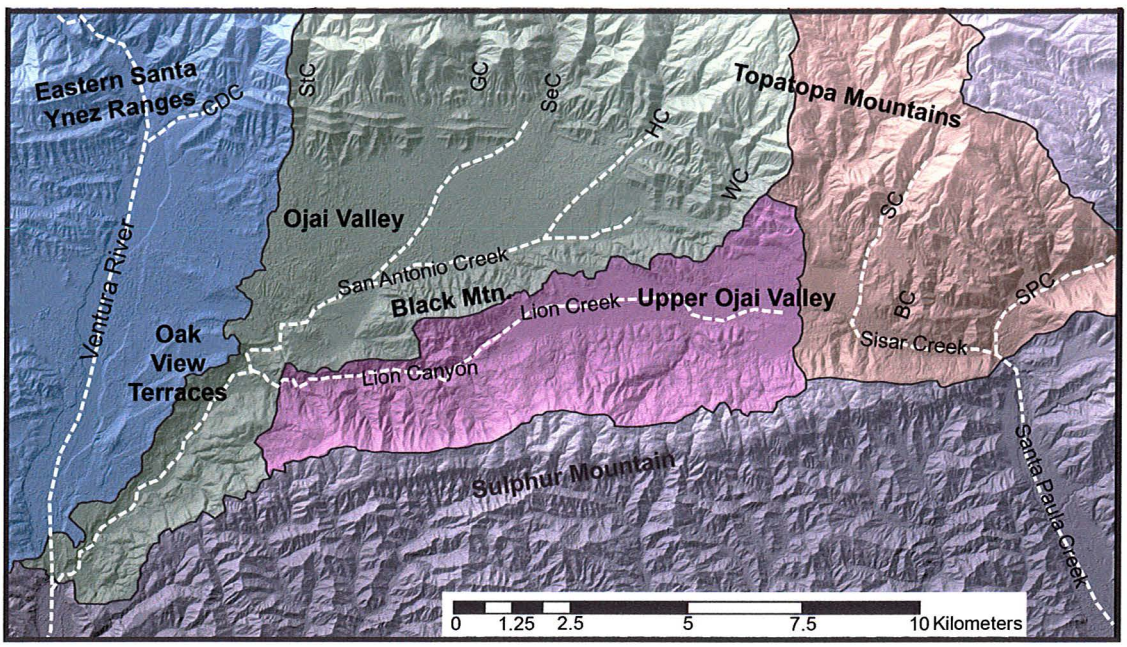

Figure 4. Map of the modern drainages (dotted white lines) with respect to Ojai and Upper Ojai valleys, drainage basins (pink- Lion Creek; green- San Antonio Creek; blue- Ventura River; and orange- Santa Paula Creek), and locations of canyons discussed in the text (CDC- Cozy Dell Canyon; StC- Stewart Canyon; GC- Gridley Canyon; SeC- Senior Canyon; HC- Horn Canyon, WC- Wilsie Canyon; SC- Sisar Canyon; and SPC- Santa Paula Canyon).

eventually the Ventura River (figure 4). Sisar Creek, also located in Upper Ojai Valley, flows southward down Sisar Canyon and then abruptly turns eastward to join Santa Paula Creek (figure 4). The eastern portion of Upper Ojai Valley is drained by Sisar Creek, which has a drainage basin area of about 45 km^2 (figure 4).

Within the study area, the bedrock is dominantly marine in origin and generally youngs to the south. In the north, the eastern Santa Ynez and Topatopa Ranges are composed of competent Oligocene-Eocene age sandstones of the Juncal, Matilija, Cozy Dell, and Coldwater Formations (figure 5 & table 1). The Oligocene age Sespe Formation underlies the majority of Ojai and Upper Ojai valleys and comprises Black Mountain (table 1 & figure 5). The Sulphur Mountain anticlinorium bounds the southern edge of the Ojai and Upper Ojai valleys and is composed almost entirely of the Monterey and Pico Formations (table 1 & figure 5). All of the bedrock is erosionally truncated and unconformably overlain by Quaternary alluvial deposits within Ojai and Upper Ojai valleys, interpreted as the Saugus Formation by previous workers (*e.g.* Rockwell *et al.*, 1984; Rockwell, 1988; Yeats *et al.*, 1988; Huftile, 1991; Huftile & Yeats, 1995) (table 1 & figure 5).

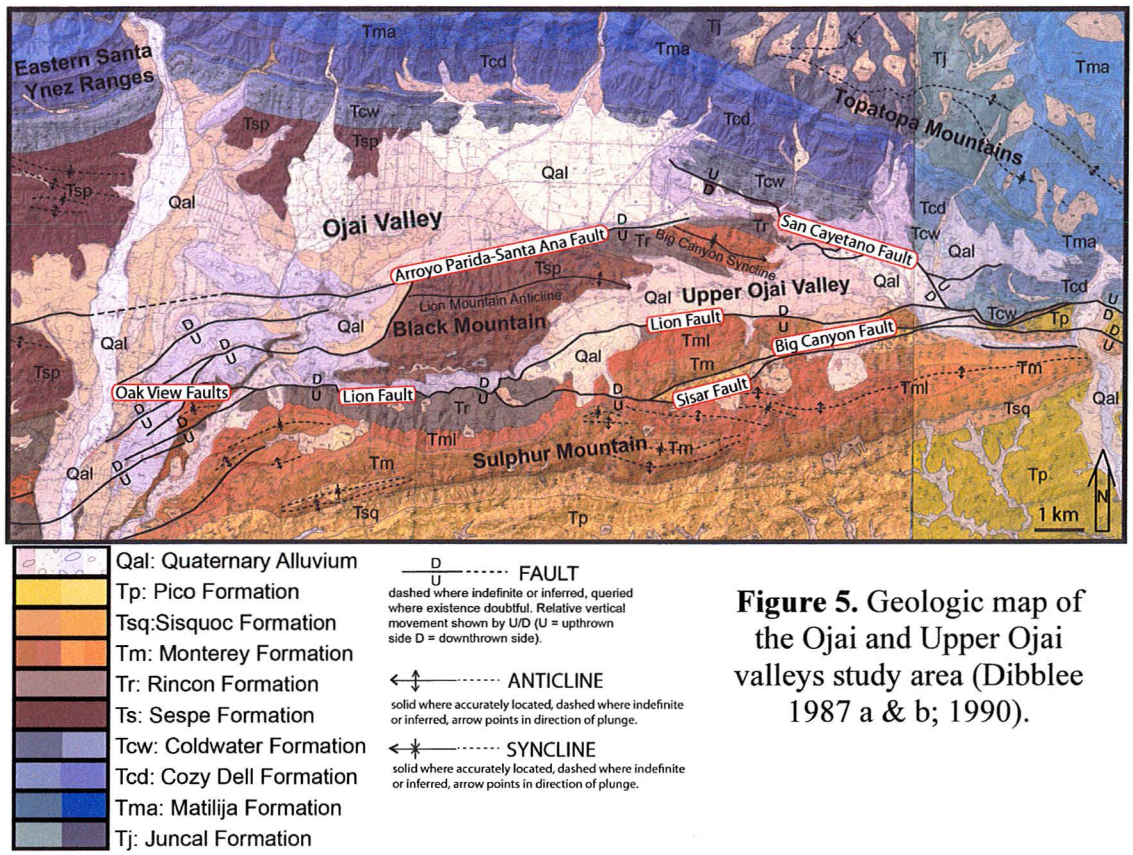

Figure 5. Geologic map of the Ojai and Upper Ojai valleys study area (Dibblee 1987 a & b; 1990).

Structures in the study area consist of roughly east-west striking reverse faults and folds that are characteristic of the wTR province (Jackson & Molnar, 1990). The westernmost surface expression of the north dipping San Cayetano fault is located at the base of the Topatopa Mountains along the northern boundary of Upper Ojai Valley (figure 5). Ojai Valley is bounded on the south by the nearly vertical Arroyo Parida-Santa Ana fault (figure 5). Big Canyon syncline and Lion Mountain anticline are exposed on Black Mountain, which separates Ojai and Upper Ojai valleys (figure 5). A series of river terraces are located to the west of Black Mountain, along the Ventura River. These terraces are named the Oak View terraces and are dissected by the Oak View faults (figure 5; Rockwell *et al.*, 1984). Lastly, surface traces of the south dipping Sisar, Big Canyon, and Lion faults are located along the northern flank of Sulphur Mountain (figure 5).

Multiple workers have calculated slip rates of active faults, estimated ages of geomorphic surfaces, and loosely constrained timing of uplift of the ranges surrounding Ojai and Upper Ojai valleys (e.g. Rockwell *et al.*, 1984; Rockwell, 1988, Huftile, 1991; Huftile & Yeats 1995). The San Cayetano fault is largely responsible for the uplift of the Santa Ynez and Topatopa Mountains. Extrapolation of modern slip rates, calculated from displaced alluvial surfaces and ages based on soil development, suggest the San Cayetano fault has been active for 1.9 Ma (Rockwell, 1988). According to Huftile (1991), folding of the Lion Mountain anticline and Reeves syncline started in the early Pleistocene and ceased prior to deposition of the basin fill in Ojai and Upper Ojai valleys. These folds have north-dipping axial surfaces and are related to early movement on a north-dipping

Era	Period	Epoch		Formation	Description
Cenozoic	Quaternary	Holocene			Alluvium: surficial sediments, landslide and talus debris, older dissected surficial sediments.
		Pleistocene Pliocene		Saugus	Nonmarine; weakly consolidated brown alluvial cobble-boulder conglomerate of poorly sorted subrounded- subangular detritus of predominantly sandstone, with minor detritus of shale, rounded granitic rocks and quartzite; crudely bedded; locally includes minor thin strata of light brown sandstone.
				Pico	Marine; massive to bedded gray siltstone, mudstone, and minor tan sandstone; sandstone locally pebbly.
	Tertiary	Miocene	L	Sisquoc	Marine; light gray silty shale or claystone, locally slightly siliceous and diatomaceous.
			M	Monterey	Marine; lower member: white-weathering, soft, fissile to punky clay shale with interbeds of hard silicious shale and thin limestone strata. Upper member: white-weathering, thin bedded, hard, platy to brittle silicious shale.
			E	Rincon	Marine; poorly bedded gray clay shale and siltstone; contains occasional gray dolomitic concretions.
		Oligocene		Vaqueros	Shallow marine transgressive; massive to poorly bedded, light gray to tan, fine grained sandstone, locally calcareous.
				Sespe	Nonmarine; maroon, red, and locally green silty shale or claystone and interbedded red to pinkish gray sandstone; some sandstone beds in lower part coarse grained and include pebble-cobble conglomerate; lowest part consists of pink sandstone and red claystone.
		Eocene	L	Coldwater	Marine; hard, tan, bedded arkosic sandstone with minor interbeds of greenish-gray siltstone and shale, includes some red siltstone; local oyster shell beds common in upper part.
				Cozy Dell	Marine; dark gray, argillaceous to silty micaceous shale with minor light gray to tan arkosic sandstone.
			M	Matilija	Marine; hard, thick-bedded, tan to mottled light greenish-gray arkosic sandstone with thin partings to thick interbeds of gray micaceous shale.
			E	Juncal	Marine; dark gray micaceous shale with minor thin interbeds of hard, gray-white to tan arkosic sandstone.

Table 1. Regional stratigraphy of the Ojai and Upper Ojai valleys study area (modified from Dibblee, 1987a & b; Dibblee, 1990; Tan *et al.*, 2005 a & b; Tan *et al.*, 2006).

blind thrust in the footwall of the San Cayetano fault (Huftile, 1991; Huftile & Yeats, 1995).

The timing of folding and faulting of the Sulphur Mountain anticlinorium is not well constrained, but according to foraminifera data from Lagoe & Thompson (1988), the middle Pliocene to middle Pleistocene Pico Member of the Fernando Formation that underlies Upper Ojai Valley was deposited as part of the main Ventura trough before uplift of the Sulphur Mountain anticlinorium. Therefore, Sulphur Mountain must be younger than middle Pleistocene. The Sulphur Mountain anticlinorium was originally a fault propagation fold and later was sequentially cut by the Big Canyon fault, Sisar fault, and most recently the Lion fault (Huftile, 1991).

In addition to the uplift history, much work has been completed on the Oak View terraces along the Ventura River. The terraces are strath terraces cut into both the basin fill and underlying bedrock. These terraces are dated between 200-100,000 years old based on radiocarbon ages and soil development (Rockwell *et al.*, 1984). The Oak View faults, which dissect the terraces, have vertical slip-rates ranging from <0.3 to 1.1 mm/yr due to flexural slip in bedding planes (Rockwell *et al.*, 1984).

Finally, previous workers have described the basin fill in Ojai and Upper Ojai valleys as coarse-grained Quaternary conglomeratic deposits (e.g. Kear, 2005; Huftile, 1991). The fill is exposed along drainages and described in numerous water-well logs as alluvial fan, floodplain, and lacustrine deposits (Kear, 2005). In Upper Ojai Valley, the fill is rarely exposed due to the downward movement of the footwall of the San Cayetano and Lion faults but has been interpreted as Saugus Formation based on oil well data (Huftile, 1991).

3. STRATIGRAPHY

3.1 Methodology

3.1.1 Field mapping

I documented sedimentology of the basin fill and its relationship with Quaternary surfaces, active structures, and underlying bedrock in Ojai and Upper Ojai valleys to elucidate the processes and timing of basin formation and filling. From August 2009 to March 2011, I conducted three weeks of field work where I described the stratigraphy of the exposed sections of basin fill, took photographs of type outcrops, measured the thickness of exposed fill, walked contacts, measured orientations of imbricated clasts, conducted clast counts, and collected samples for geochronology. These data were compiled to make a series of figures that document the stratigraphy, lithology, three-dimensional geometry, and age of the basin fill within Ojai and Upper Ojai valleys.

I carefully mapped the lateral extent of the basin fill using a 3m digital elevation model, topographic maps, and aerial photography as a base. In addition, aerial photos viewed in stereo and geologic maps (e.g. Dibblee, 1987a & b; Dibblee, 1990; Tan *et al.*, 2005a & b; Tan *et al.*, 2006) aided in the mapping of geologic and geomorphic features.

3.1.2 Outcrop descriptions, clast counts, & measurement of imbricated clasts

Sedimentologic observations were used to constrain the depositional environment, source, lithology, and direction of paleodrainage within the basin. I took photographs of type exposures to document the variable characteristics of the deposits. In Lion Canyon, a Brunton compass and measuring tape were used to measure the only accessible exposed section. Clast counts were made at the top, middle and bottom of the measured section as well as an additional eight clast counts at outcrops that expose the base and lower portions of basin fill and in each of the active drainages.

At each clast count location a horizontal measuring tape was laid out and the size, color, and composition of clasts at 10 cm intervals were recorded. Approximately 30 clasts were measured in every location. Thus, the values are presented as percentages in pie charts. The lithologies of the clasts are compared with the lithologies of the bedrock that comprise the surrounding ranges to interpret the source of the sediments that filled the basins. Clast counts in active channels are used to document the lithologies of clasts that are actively being transported downstream.

The orientations of at least 20 cobble-size imbricated clasts were also measured at each location. The orientations of the clasts were plotted on lower hemisphere stereonets, and then the poles to the planes were calculated and plotted. From these stereonets, the down-plunge azimuths were plotted on rose diagrams. The directions on the rose diagrams represent the direction of flow when the sediments were deposited. From these data, the basin fill was separated into seven lithofacies that document the different processes responsible for filling the basins.

3.1.3 Subsurface data

Subsurface data from previous workers (*e.g.* Huftile, 1991; Kear, 2005; Ventura County Flood Control District) and thicknesses of exposed sections were combined to

create an isochore map that shows the true vertical thickness of the basin fill. Subsurface data for Ojai Valley, the Ventura River floodplain, and along San Antonio Creek was calculated from a contour map of the effective base of the ground water reservoir created by the Ventura County Flood Control District. The contour map is controlled by at least 30 water wells. Additional data from water wells in Ojai Valley from Kear (2005) were also incorporated into the isochore map. Thickness data for Upper Ojai Valley is based on a cross section and three oil wells from Huftile (1991).

3.1.4 Absolute dating

Two absolute age dating methods were attempted to constrain the age of the basin fill. In-situ $^{26}Al/^{10}Be$ cosmogenic burial dating was used to find the age of the base of the fill. Two samples were collected and analyzed. Radiocarbon dating was used to find the age of the uppermost fill in Upper Ojai Valley. Six samples of charcoal were collected from the outcrop, two of which were analyzed.

$^{26}Al/^{10}Be$ cosmogenic burial dating

Quartz is exposed to cosmogenic nuclides ^{26}Al and ^{10}Be when it is near or on the surface of the Earth (Lal, 1991; Granger & Smith, 2000). The production ratio ($^{26}Al/^{10}Be$) remains constant at ~6 regardless of sample location (Lal, 1991). When sediments are subsequently buried 20-30 m deep, production of cosmogenic nuclides ceases (Granger & Smith, 2000) and ^{26}Al and ^{10}Be begin to decay exponentially based on their relative half lives ($t_{1/2}$ Al = 7.17×10^5 years, Norris *et al.*, 1983; $t_{1/2}$ ^{10}Be = 13.7×10^5 years, Nishiizumi *et al.*, 2007). The time since sediment burial can be back calculated from the current $^{26}Al/^{10}Be$ ratio (Granger & Muzikar, 2001). This technique has proven successful in finding the age of cave deposits and thick, Plio-Pleistocene sedimentary formations (e.g., Stock *et al.*, 2004; Balco *et al.*, 2005; Kong *et al.*, 2009) and has been shown to be effective over a range 0.1 and 5.0 Ma.

In this study, two samples were collected following techniques by Granger *et al.* (2001). They were prepared based on methods described in Kohl & Nishizumi (1992). Mineral digestion, column chromatography, and target packing were completed by Richard Heermance at the University of California Santa Barbara Cosmogenic Radionuclides Target Preparation Facility, which is operated by Bodo Bookhagen. Acceleration Mass Spectrometry (AMS) analysis was performed at the Lawrence Livermore National Laboratory Center.

Radiocarbon dating

Conventional radiocarbon dating on detrital charcoal is widely used to find the age of sedimentary deposits and provides maximum ages because charcoal dates represent the time of wood growth, which is always older than the time of deposition (*e.g.* Madden *et al.*, 2006; Delong & Arnold, 2006; Villani, 2010). In this study, six samples were collected from the organic rich sediments in Upper Ojai Valley and two were analyzed.

Paul McBurnett prepared two targets for AMS dating at the W.M. Keck Carbon Cycle Accelerator Mass Spectrometry Laboratory at University of California, Irvine. Radiocarbon concentrations are given as fractions of the modern standard, $D^{14}C$, and conventional radiocarbon age. They are corrected for isotopic fractionation, following the

conventions of Stuiver & Polach (1977). Conventional radiocarbon ages were calibrated using OxCal v4.1.7, which uses calibration curves from Bronk Ramsey (2010) and atmospheric data from Reimer *et al.* (2009).

3.2 Data & observations

3.2.1 Stratigraphic descriptions

In this study, every outcrop of the basin fill in Ojai and Upper Ojai valleys was described (table 2) and then separated into different deposits in order to document the processes of basin filling (figure 6). The deposits are separated into different facies, which are bodies of rock with specified characteristics that reflect a particular process or environment. The facies in this study are based on sedimentology, lithology, and outcrop locations for each of the deposits (table 2; figure 6). The majority of the outcrops of the basin fill are composed of conglomerates.

In addition to descriptions of outcrops, a stratigraphic section was measured in Lion Canyon. Near vertical incision of Lion Canyon provides excellent exposures of the basin fill. The type-measured section (figure 7) consists of steeply dipping (at least 55°) Tertiary age strata overlain by up to 60 m of facies C1. In a few areas, the Quaternary strata are tilted up to 15°. Clast counts were conducted at several intervals throughout the section. Clasts at the base and middle of the section are composed almost entirely of tan, grey, tan, buff and brown-colored sandstones. Rare clasts of red sandstone are present throughout the section. Clasts of white diatomaceous shale are incorporated in the upper 10-15 m of section, as evident by the clast count closest to the top.

3.2.2 Clast counts & imbrication

In this study, clast counts are used to document the lithology of the clasts in the basin fill of Ojai and Upper Ojai valleys. The dominant lithology in all of the clast counts, both in the outcrops and active channels, is grey, tan, buff, and brown-colored sandstones (figure 8; figure 6a, b, & e). The majority of the clast counts also measured a few red-colored sandstone clasts (figure 8). All of the measured sandstone clasts were medium or coarse grained. In a few locations, igneous and metamorphic clasts were present (figure 8). The only clast count containing white diatomaceous shale is in the uppermost clast count in the measured section from Lion Canyon (figure 7) but this lithology was observed in the same stratigraphic position in multiple other locations throughout Lion Canyon.

The diameters of the clasts were also recorded in the clast counts (table 3). The smallest average clast size, 6.8 cm diameter, is at the top of the measured section (figure 7; table 3). On the other hand, the largest average clast size, 22.4 cm, is at Meditation Mount (clast count 08 on figure 8; table 3).

Imbricated clasts were measured at each of the outcrops in order to infer the paleocurrent direction of the paleodrainage system at the time of deposition. Two of the three locations of imbricated clast measurements along the Ventura River have clasts oriented so that the paleoflow was to the south (figure 9). In the central portion of the field area, the three of the four locations of imbricated clast measurements are oriented so that the paleoflow was to the northwest (figure 9).

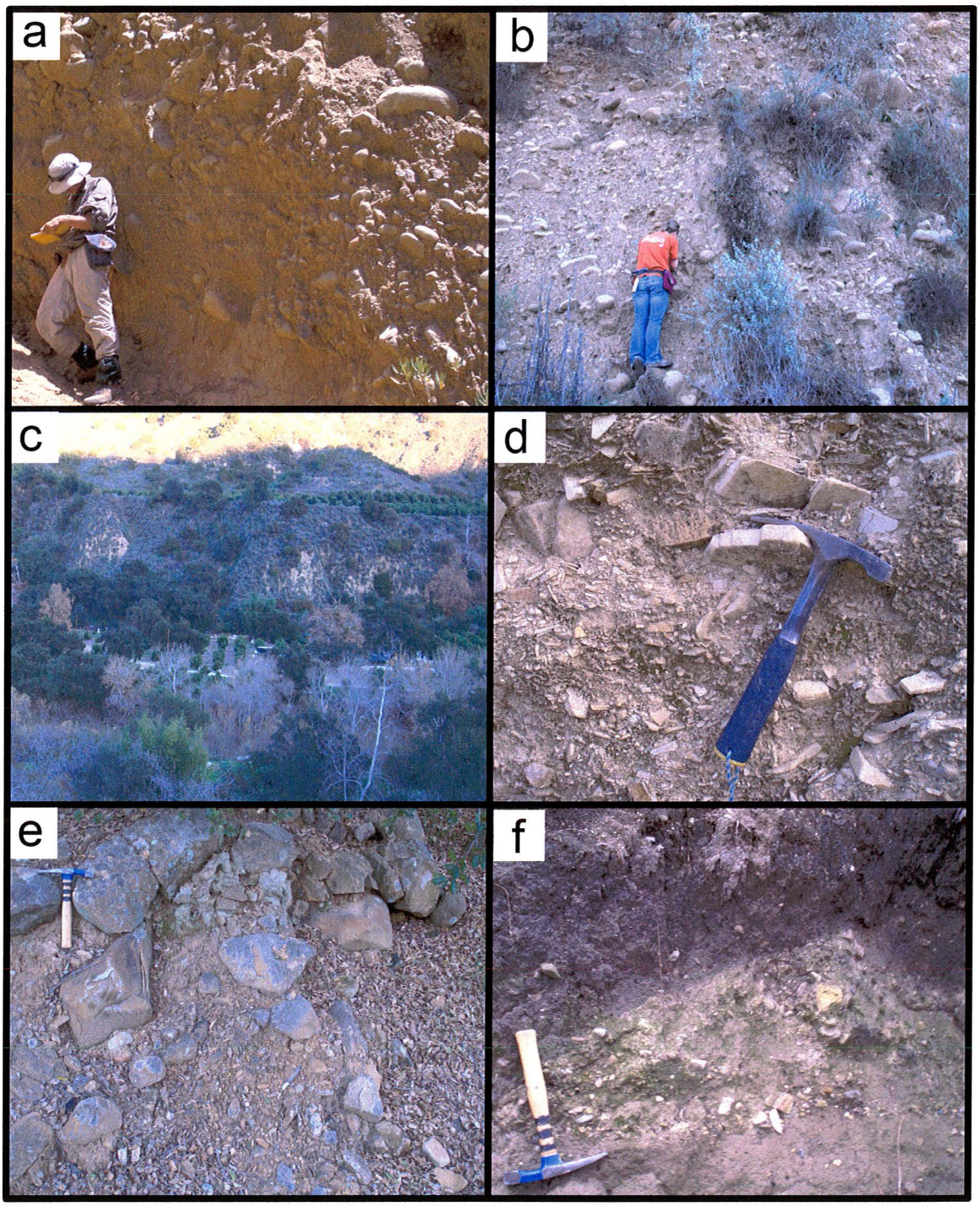

Figure 6. Photographs of type outcrops of the basin fill in Ojai and Upper Ojai valleys, note people and rock hammer for scale. Sedimentologic descriptions of outcrops are in table 2 and locations of photographs are shown in figure 8. (a) Pebble to boulder conglomerate with discontinuous sands typical of facies C1 in Lion Canyon; (b) Typical thickness on consolidation of facies C1 in eastern bank of Ventura River; (c) Fill terraces along Santa Paula Creek composed of facies C3, entire height of photograph is ~20 m; (d) Angular to sub-angular clasts composed of white diatomaceous shale typical of facies C4; and (f) Dark brown muds and matrix supported conglomerate of facies L1.

Facies	Stratigraphic Description	Locations of Outcrops
C1	Very poorly sorted, dominantly clast-supported, pebble-boulder conglomerate. Clasts are subrounded, composed of dominantly competent tan, grey, and buff sandstone, and are commonly imbricated. The matrix consists of very poorly sorted silt to very coarse sand-sized particles. Stratification is generally lacking, but outcrops commonly contain some 0.5-1 m thick gravel-rich intervals separated by boulder-rich layers. Rare lenses, 0.25-0.5 m thick and several m long, and laterally discontinuous layers composed of moderately sorted, coarse sand-pebble sized material are rare (figure 6a). When visible, the basal contact is an angular unconformity with highly deformed Eocene-Miocene age strata (table 1). Typical deposits are several m to tens of m thick and well consolidated (figure 6b).	Facies C1 crops out along the Ventura river where the Oak View terraces are cut into the deposits and in the walls of Lion canyon.
C2	Poorly sorted, clast-supported, pebble-cobble conglomerate (figure 6c). Clasts are subangular and composed of dominantly sandstone. The matrix is dark brown fine-medium sized sand. Outcrops are moderately consolidated.	Facies C2 crops out in fill terraces located along Santa Paula Creek.
C3	Poorly sorted, matrix-supported, pebble-cobble conglomerate. Clasts are angular and composed entirely of white platy shale. Matrix is poorly sorted and composed of silt to medium sand sized material. Outcrops are generally unconsolidated (figure 6d).	Fan-shaped deposits located on the north flank of Sulphur mountain, predominantly along the southern edge of Upper Ojai valley are composed of facies C3.
C4	Very poorly sorted, matrix- and clast-supported, weakly consolidated pebble-boulder conglomerate. Clasts are subrounded, composed of entirely tan, gray, and buff colored sandstone, and 0.5-2 m diameter boulders are common. When present, the matrix is very poorly sorted, fine sand to coarse sand-sized material. Deposits are unconsolidated (figure 6e). Orchards of orange trees usually grow in facies C4.	Outcrops are located in fan shaped deposits at the base of the eastern Santa Ynez range and Topatopa mountains in the northern portion of the study area.
L1	Poorly consolidated dark yellowish brown (10YR 4/2) silty muds (figure 6f). At least one very irregular, 10-50 cm thick, layer of matrix-supported, very coarse sand-pebble conglomerate is present. The top of the conglomeratic layer is undulating. Clasts are polymict, both subangular and rounded with occasional angular to subangular clasts composed of white shale, black, red and grey chert, and surrounding brown muds. Multiple lenses filled with clast supported subangular, poorly sorted, pebble-coarse sand conglomerates are present. The matrix in the channels is greyish brown (5YR 3/2) and composed of sand sized material. Channels vary in size and are 0.25-0.5 m thick and up to several m wide. No orchards present where the L1 facies is on the surface.	Facies L1 crops out along Lion creek in Upper Ojai valley and is bounded by landslides in the west.
LS1	Landslide and slump deposits. In the majority of the localities, a head scarp is present and lobate toes are less common.	Landslides are common in the steeper topography composed of the non-competent formations (table 1). Many of the deposits are in close proximity to active faults.
A1	Unconsolidated, poorly sorted alluvium	Active channels

Table 2. Facies, sedimentologic descriptions and locations of outcrops of the basin fill in Ojai and Upper Ojai valleys.

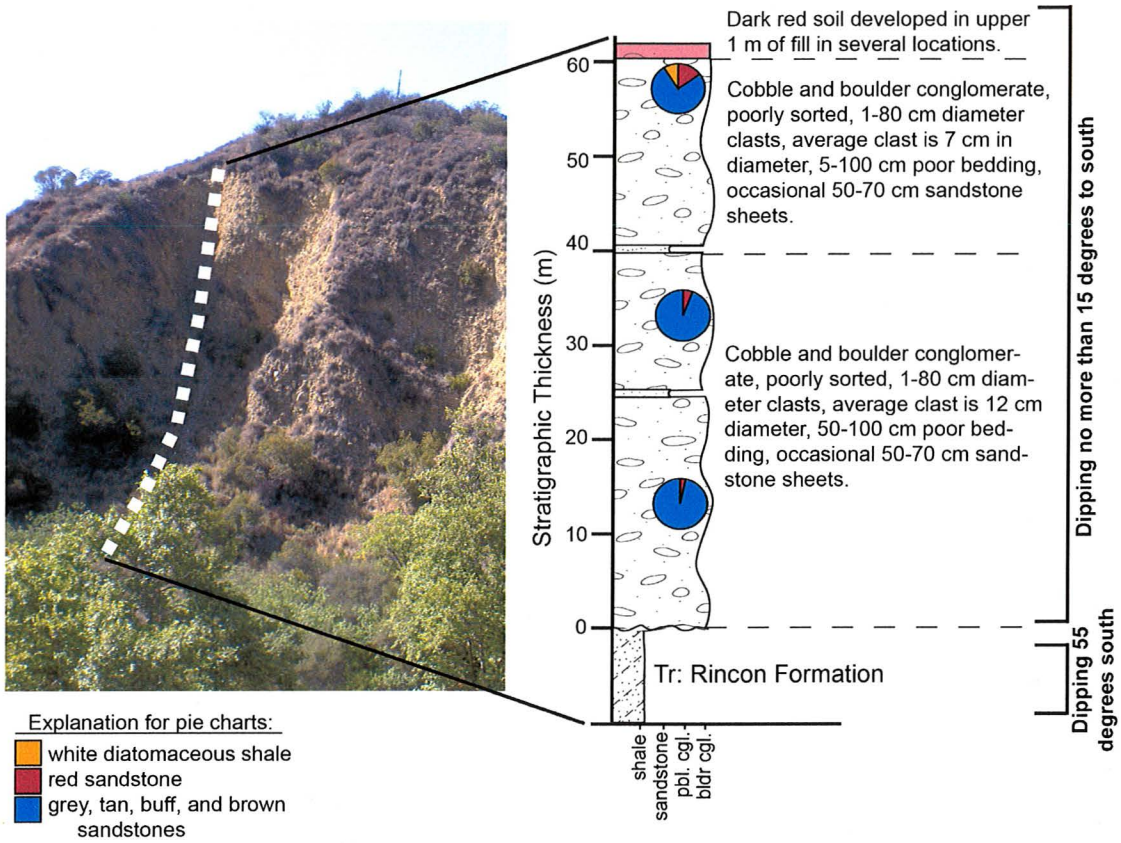

Figure 7. Photograph, measured section, description, clast count data, and structure of the basin fill in Lion Canyon.

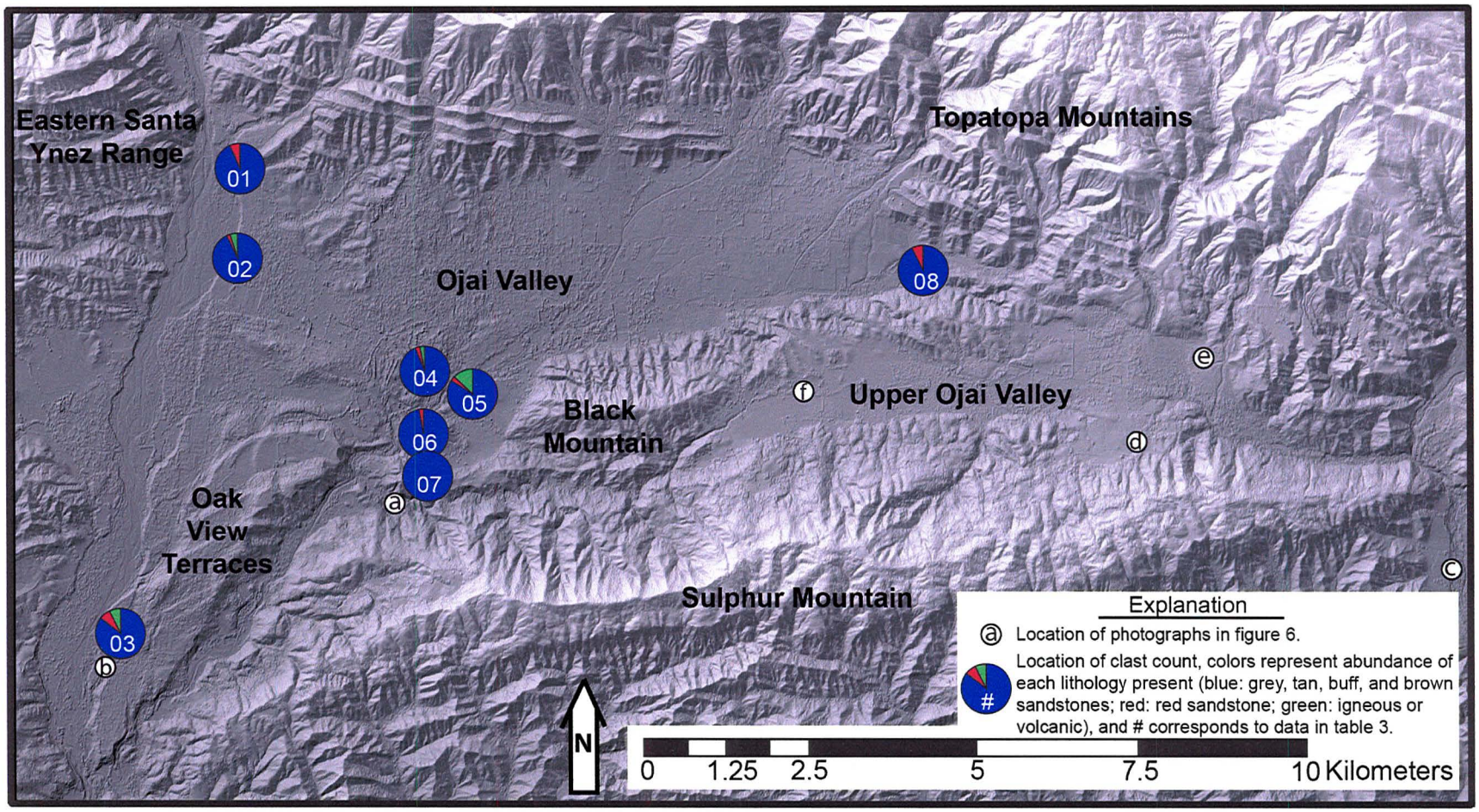

Figure 8. Map of the Ojai and Upper Ojai valleys with pie charts in locations of clast counts from the lowest exposed sections of basin fill. Additional clast count data are in table 3. Locations indicated by a-f are type outcrops of the basin fill that are pictured in figure 6.

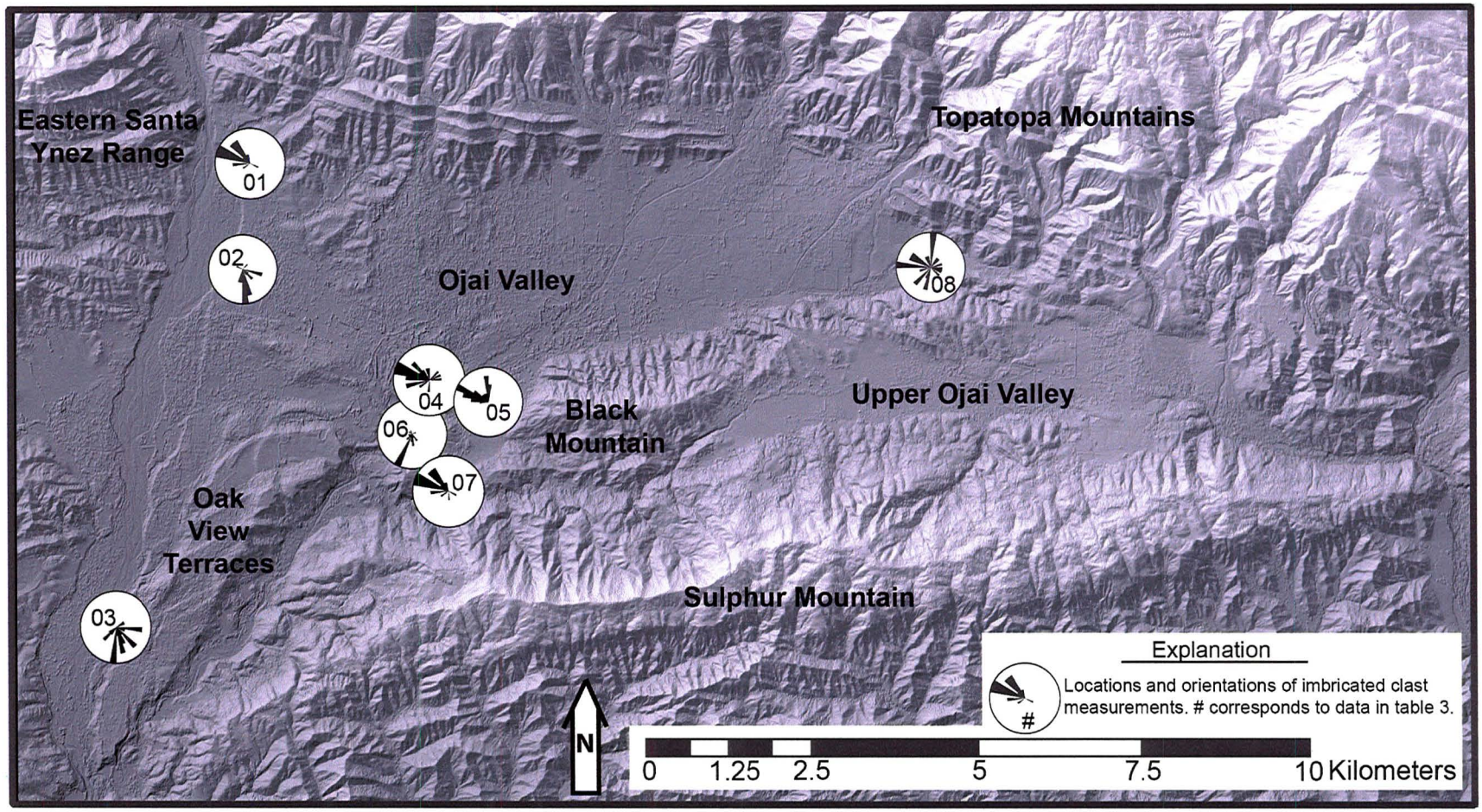

Figure 9. Map of the Ojai and Upper Ojai valleys with rose diagrams that show the orientation of measured imbricated clasts. Additional imbricated clast data are in table 3.

Table 3. Additional clast count and imbricated clast data for figures 7-9. The "% represented by outer circle of the rose diagrams" is calculated from the mode azimuth at each location divided by the number of measured imbricated clasts at each location. Note that the outer circle represents a different percentage at each location.

	Location description	# of clasts in clast count	Average clast diameter	# of measured imbricated clasts	% Represented by outer circle of rose diagram	Average azimuth direction
Figure 8	Vru- Active channel- Ventura River, upstream	41	10.6 cm	Not measured		
	Vrl- Active channel- Ventura River, downstream	30	11.4 cm			
	SAC- Active channel- San Antonio Creek	32	17.0 cm			
	LC- Active channel- Lion Creek	23	20.6 cm			
Figure 7	Top of measured section	33	6.8 cm			
	Middle of measured section	34	10.7 cm			
	Bottom of measured section	36	12.4 cm			
Figures 8 & 9	01- east bank of Ventura River	30	8.3 cm	22	18	211
	02- east bank of Ventura River	42	9.0 cm	22	23	161
	03- east bank of Ventura River	27	9.7 cm	26	16	152
	04- west bank of San Antonio Creek	32	7.0 cm	21	14	254
	05- east bank of San Antonio Creek	31	8.8 cm	22	18	158
	06- Camp Comfort	34	10.7 cm	28	32	204
	07- Lion Canyon	28	5.3 cm	23	18	318
	08- Meditation Mount	27	22.4 cm	25	12	287

3.2.3 Fill thickness

Basin fill is thickest in the center of the eastern portion of Upper Ojai Valley (> 500 m) (figure 10). The fill thins to approximately 300 m to the north and about 200 m to the south before abruptly terminating against the San Cayetano and Lion faults, respectively (figure 10). Due to lack of subsurface data, the fill has been interpreted to gradually thin into the western portion of Upper Ojai Valley and pinch out onto Black Mountain (figure 11). There is no evidence that basin fill to ever covered Black Mountain.

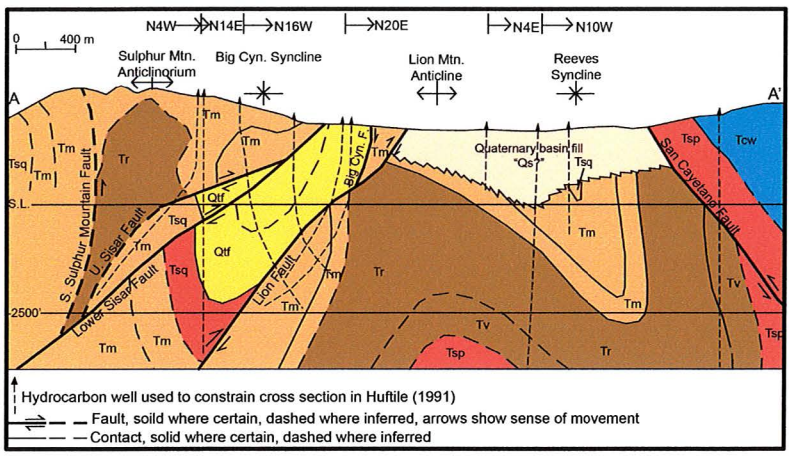

Figure 10. Cross section A-A' across Upper Ojai Valley (modified from Huftile (1991). Location of cross section shown in figure 11 (note that figure 10 & 11 are at different scales). Refer to figure 3 for formation abbreviations and colors.

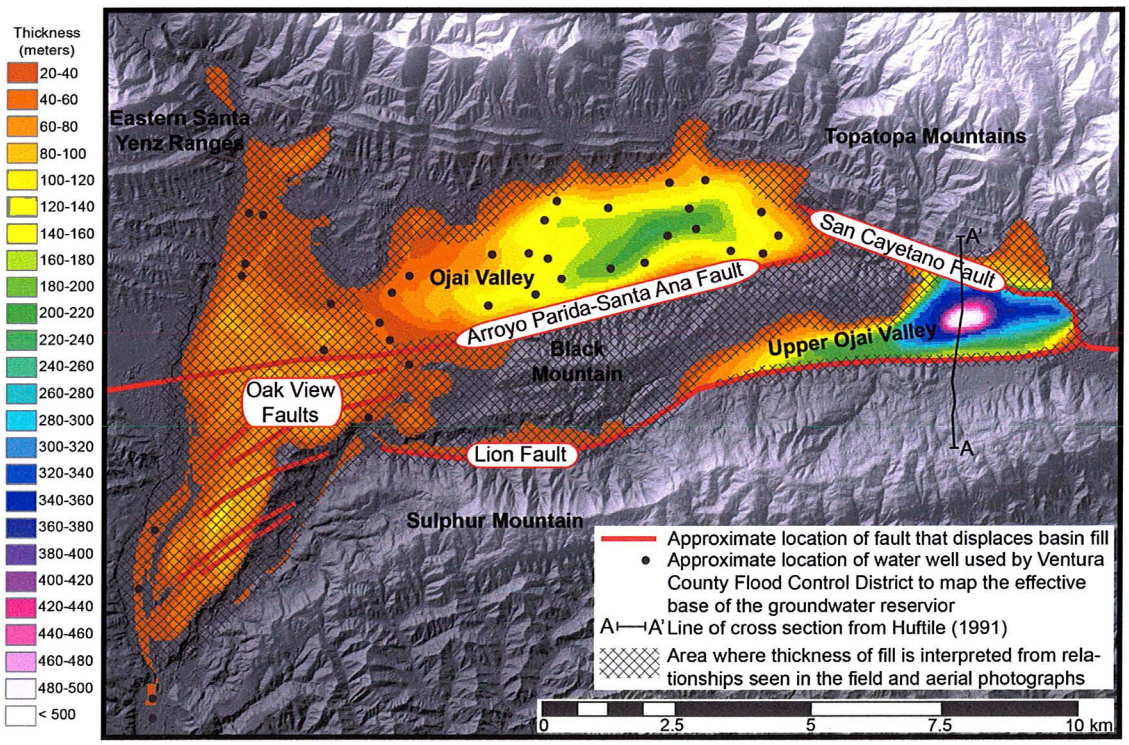

Figure 11. Isochore map of the true vertical thickness of the basin fill in Ojai and Upper Ojai valleys including surface locations of faults that displace the basin fill.

The basin fill reaches a maximum thickness of 240 m in the eastern part of Ojai Valley, just north of the Santa Ana fault (figure 11). The fill thins gradually to the north toward the base of the Topatopa Mountains. To the west, the fill also thins to approximately 20 m before again thickening to approximately 100 m beneath the Ventura River. In the area to the south of the Santa Ana-Arroyo Parida fault, the fill ranges in thickness from 0-120 m below the surfaces of the Oak View terraces. The fill is up to 40 m thick in Lion Canyon and sporadic clasts are present on Sulphur Mountain, above the current fill.

3.2.4 Geochronology

The relative age of the basin fill is constrained by the age of the folded and faulted bedrock below the basin fill and the age of a series of at least four fluvial terraces preserved along the Ventura River that are cut into the basin fill (figure 4 & 12). The youngest bedrock underlying the basin fill in Upper Ojai Valley is the middle Pliocene to middle Pleistocene Pico Member of the Fernando Formation (figure 10, table 1), which provides the maximum age for the fill. Radiocarbon dating and soil chronology estimate that the terrace surfaces are 30 to 92 ka (figure 12; Rockwell *et al.,* 1984). However, the age of the 15-20 ka terrace (Qt5a in Rockwell *et al.,* 1984) is based on a radiocarbon date from the Ventura area and a cosmogenic depth profile suggests an age of only ~6-7 ka (D. DeVecchio *et al.*, in press). The ^{14}C age of ~38 ka for Qt6a is not calibrated (Qt6a in Rockwell *et al.,* 1984) but based on calculations using OxCal v4.1.7, the calibrated age

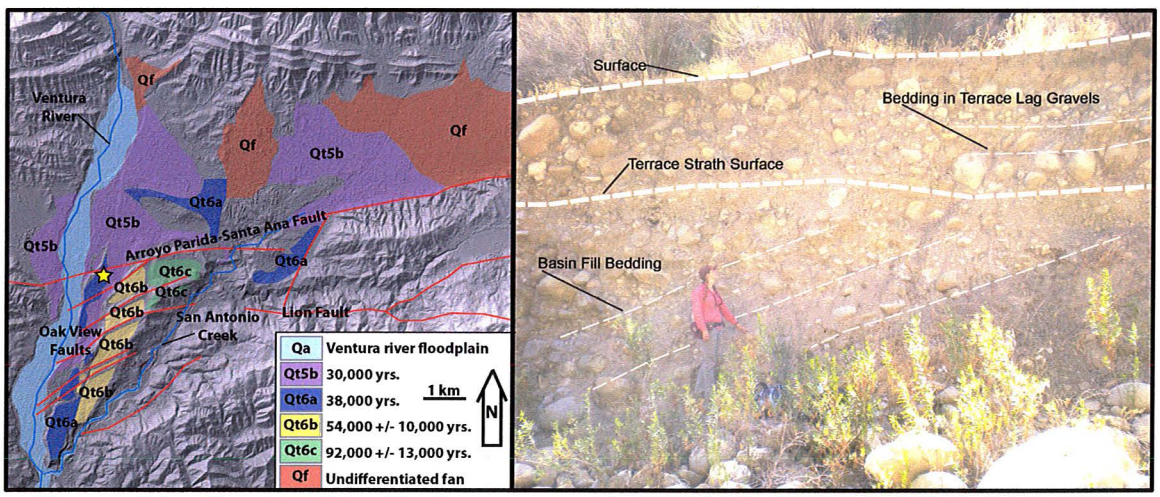

Figure 12. Map of terrace surfaces in Ojai area (left; Rockwell *et al.,* 1984 and photograph of a terrace at the base of Lion Canyon that show the relationship between basin fill and terrace surfaces (right). The yellow star on the map is the location where the vertical slip rate for the Arroyo Parida-Santa Ana fault because it displaces terrace surface Qt6a. The photograph on the right shows that the terrace is composed of tilted basin fill overlain by horizontally bedded terrace gravels above the terrace strath. Note author for scale.

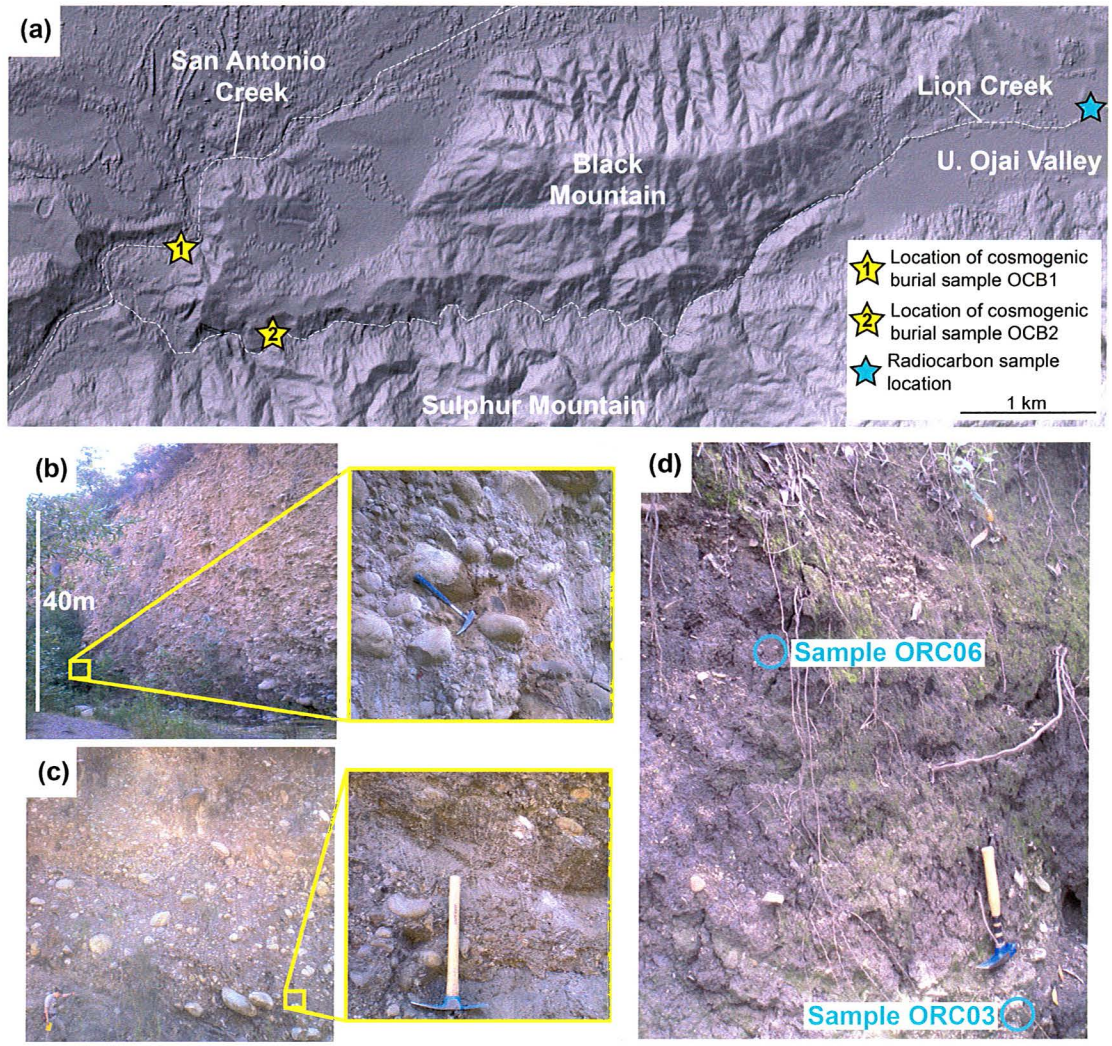

Figure 13. Map and photographs showing the locations of geochronology sampling in Ojai and Upper Ojai valleys. (a) Map of Ojai and Upper Ojai valleys with white dotted lines showing locations of drainages. Stars indicate locations of cosmogenic burial and radiocarbon sampling. (b) Photographs of location of collection of Ojai cosmogenic burial sample 1 (OCB1). Photograph of outcrop (left) and actual sample site (right), note rock hammer for scale. (c) Photographs of location of collection of Ojai cosmogenic burial sample 2 (OCB2). Photograph of outcrop (left), note author for scale, and actual sample site (right), note rock hammer for scale.

for this terrace is 42,252 ± 1,233 years B.P., which agrees with the cosmogenic exposure age based on sampled boulders (DeVecchio *et al.*, in press). Therefore, formation of the Oak View terraces along the Ventura River occurred between ~92 and 6 ka, and the basin fill is younger than middle Pleistocene and older than all of the terrace surfaces. To better constrain this age, $^{26}Al/^{10}Be$ cosmogenic burial and radiocarbon dating techniques were used.

$^{26}Al/^{10}Be$ cosmogenic burial dating

Two samples were collected from the base of the basin fill for cosmogenic radionuclide age-dating analysis. Sample OCB1 (Ojai Cosmogenic Burial #1) was collected from the exposed basal contact along San Antonio Creek at Camp Comfort (figure 14), A second sample, OCB2, was collected nearly 3 km to the south, within Lion Canyon, where the Lion fault displaces and exposes the basal contact (figure 14).

Concentrations of ^{26}Al and ^{10}Be were determined for the two samples and the results are displayed in table 4. AMS analysis of the ^{26}Al targets resulted in extremely low counts (less than background) and thus large uncertainties (20-40%) before background correction. An Al blank was not run so a background correction cannot be completed. Additionally, the ^{10}Be currents obtained from the AMS analysis were low (< 1 microamp), contributing to high errors and low precision results. These low values could be due to sample contamination, analytical error, and/or too young of samples but the data is too uncertain to use. Sample ages, calculated using techniques described by Granger & Muzikar (2001), are displayed for completeness but they were not used in this study.

Table 4. Cosmogenic sample information and related data from AMS analysis.

Sample	Mass quartz (g)	Be carrier (mg)	Al carrier (mg)	$^{10/9}Be$ ratio ±1σ error	^{10}Be conc. (atoms/g) ±1σ error	$^{26/27}Al$ ratio ±1σ error	^{26}Al conc. (atoms/g) ±1σ error	Prod. ratio ($^{26}Al/^{10}Be$)	Age (Ma)
OCB01	121.314	0.4379	n/a	$9.29 \times 10^{-14} \pm 1.93 \times 10^{-15}$	$2.07 \times 10^{4} \pm 7.12 \times 10^{2}$	$2.487094\ 5 \times 10^{-14} \pm 7.289925 \times 10^{-15}$	$5.234475 \times 10^{4} \pm 1.534277 \times 10^{4}$	2.53	1.83
OCB02	77.46	0.4364	n/a	$4.59 \times 10^{-14} \pm 1.90 \times 10^{-15}$	$1.45 \times 10^{4} \pm 8.49 \times 10^{2}$	$1.347651 \times 10^{-14} \pm 4.957575 \times 10^{-15}$	$3.436448 \times 10^{4} \pm 1.264158 \times 10^{4}$	2.36	1.98

Radiocarbon dating

Six detrital charcoal samples of facies L1 (table 2 & figure 6f) were collected for radiocarbon analysis from the bank of Lion Creek where it has incised into the fill in Upper Ojai Valley (figure 12). Upon further inspection, some of the samples were in fact not charcoal. Furthermore, due to limited funding, only two samples were processed. Sample ORC03 was collected from the lowest exposed conglomeratic bed and sample ORC06 is a bulk sample collected from the dark brown mud that overlies the conglomerate (figure 12). The sample locations are separated by ~ 0.75 m of section.

The calibrated age of sample ORC06, within 2σ uncertainty, is 14,865 ± 365 years calBP (table 5 & figure 14a). Calibration curves end at 50,000 calBP because this age is near the maximum range applicable for the technique due to the very small amount of remaining measureable carbon. With the associated error, the ^{14}C age for sample ORC03 could be greater than 50,000 BP and the resulting calibrated age is greater than 46,372calBP (table 5 & figure 14b).

Table 5. Dates and descriptions of radiocarbon samples from facies L1 in Upper Ojai Valley.

Sample Name	Description	Fraction Modern	$D^{14}C$ (‰)	^{14}C age (years B.P.)	Calibrated Age (Cal. years B.P.)
ORC06	Detrital charcoal (0.10 mg C)	0.2077 ± 0.0014	-792.3 ± 1.4	12,630 ± 60	14,865 ± 365
ORC03	Bulk sample	0.0033 ± 0.0007	-996.7 ± 0.07	46,000 ± 1800	> 46,372

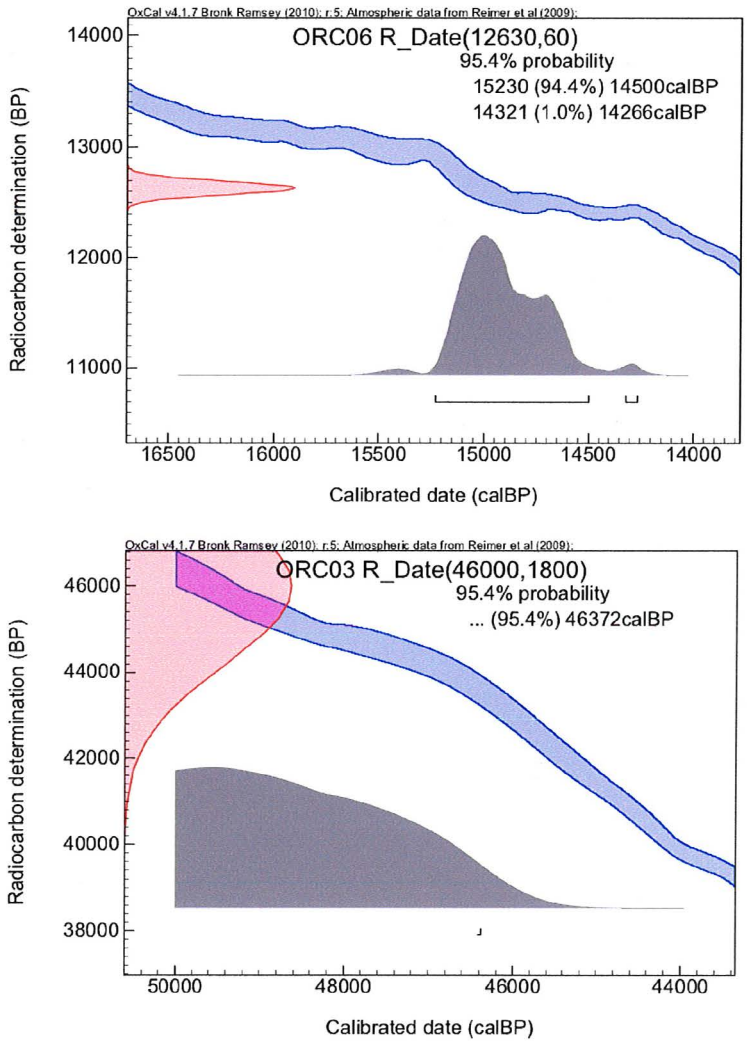

Figure 14. OxCal v4.1.7 graphs for radiocarbon samples that show calibration curves (blue), probability distributions of ^{14}C ages (red), and probability distributions of the calibrated ages (grey). (a) Top- sample ORC06 and, (b) bottom- sample ORC03.

3.3 Interpretations

3.3.1 Depositional setting

Facies C1

The rounded clasts, clast-supported nature of the deposits, imbrication, and sand bodies lacking clay-size material in facies C1 indicate deposition by streamflow, whereas the poor stratification, presence of boulder-size clasts, poor sorting, and lack of sedimentary structures suggest deposition by debris flow (Middleton & Hampton, 1976; Nilsen, 1982; Boggs, 2006). Due to these characteristics, I interpret facies C1 to represent fluvial gravels deposited in a braided channel system (Nilsen, 1985; McLane, 1995). The coarse grain size and poor sorting are indicative of high-energy environments, which suggest that deposition occurred primarily during floods (Boggs, 2006).

Facies C2

The subrounded clasts and clast-supported nature of facies C2 suggest deposition in a fluvial environment. Alternatively, the lack of sedimentary structures and poor sorting are evidence that deposition was high energy. These characteristics suggest that facies C2 was deposited in a braided channel complex (Middleton & Hampton, 1976; Boggs, 2006). The stream likely had a steep gradient, very similar to the modern Santa Paula Creek.

Facies C3

The poor sorting, angular clasts, and immature compositions of clasts in facies C3 are representative of a proximal alluvial fan (Nilsen, 1982). This interpretation is consistent with their fan-shaped geomorphology where the apex of the fan is located at the mountain front (figure 15; Blair & McPherson, 1994). Poorly sorted and matrix-supported conglomerates are common in debris flows on proximal alluvial fans (Middleton & Hampton, 1976; Nilsen, 1982). Also, it appears that the clasts of white shale decrease in size rapidly, rather than rounding so they are only found in close proximity to Sulphur Mountain.

Facies C4

Facies C4 represents sediments deposited in proximal alluvial fans derived from the eastern Santa Ynez and Topatopa ranges to the north of Ojai and Upper Ojai valleys. Debris flows and sieve deposits, which are rapidly deposited gravel lobes, are common in proximal alluvial fan settings (Nilsen, 1982; Boggs, 2006). The deposits are fan-shaped where the apex of the fan is located at the mountain front (figure 15; Blair & McPherson, 1994).

Facies L1

The laterally continuous sequence of mud, sand, and conglomerate beds in facies L1 is typical of sediments deposited within a marginal lacustrine environment (Fouch & Dean, 1982). The irregular layers of matrix supported conglomerate represent debris flows washing into the lake, which suggests steep topography. Along the lake margins, channelized conglomerates are similar to channels in the Pliocene Ridge Basin Group

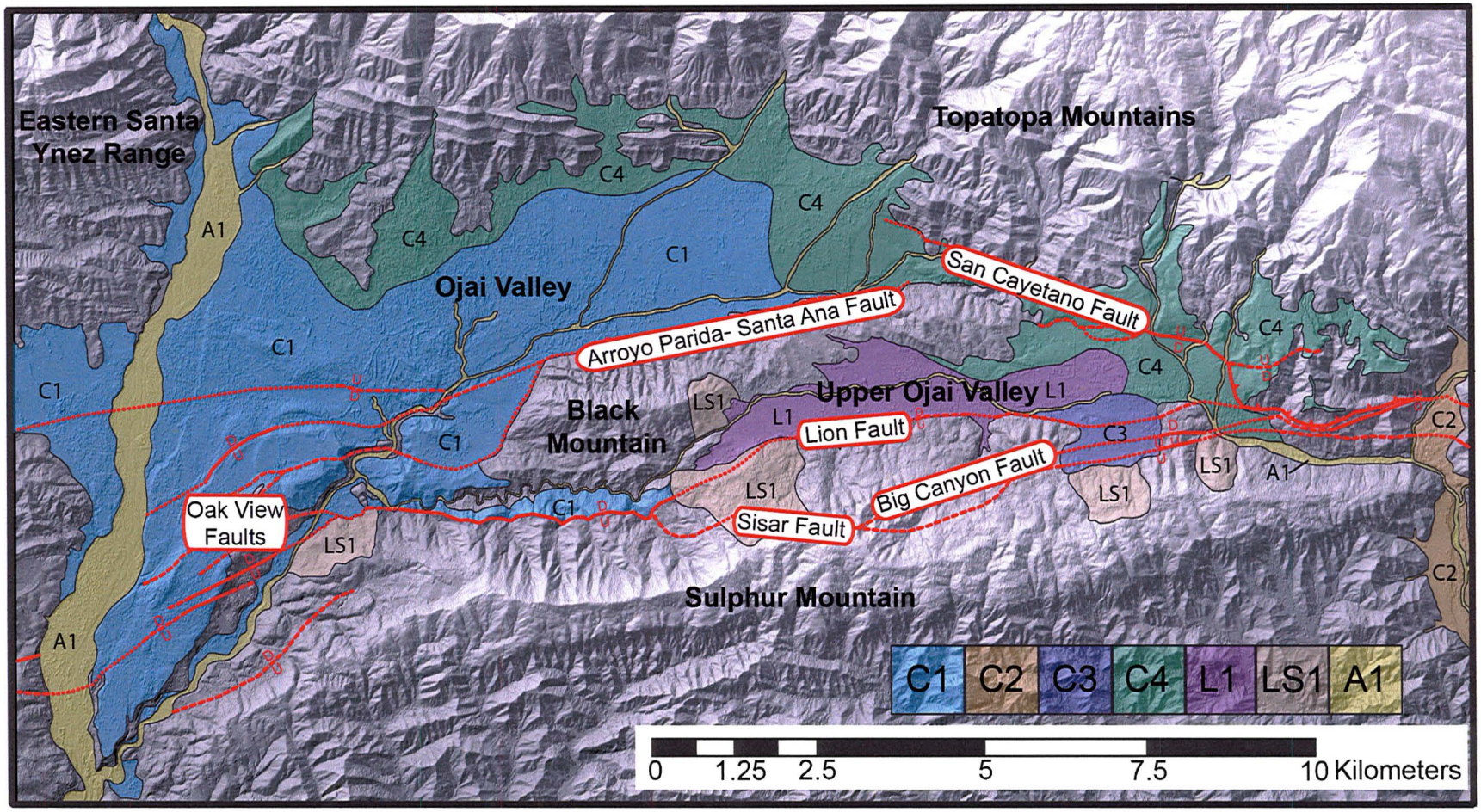

Figure 15. Lithofacies of the basin fill in Ojai and Upper Ojai valleys characterized by depositional setting, lithology, and locations of outcrops. Red lines are surface locations of faults that displace basin fill with U/D showing relative movement. Faults are solid where certain, dashed where inferred, and dotted where concealed.

Table 6. Summary of lithofacies in the basin fill of Ojai and Upper Ojai valleys

Facies	Description	Interpretation
C1	Well consolidated, clast-supported, subrounded, pebble-boulder conglomerate	Fluvial gravels within a braided channel system
C2	Moderately consolidated, clast supported, subangular, pebble-boulder conglomerate	Immature braided stream deposits
C3	Matrix-supported, angular, pebble-cobble conglomerate with white shale clasts	Proximal alluvial fan deposits sourced from Sulphur Mountain
C4	Slightly consolidated, matrix- and clast-supported, pebble-boulder conglomerate	Proximal alluvial fan deposits sourced from the eastern Santa Ynez Ranges and Topatopa Mountains
L1	Poorly bedded, dark brown silty muds and channels filled with pebble conglomerates	Lacustrine
LS1	Landslides and slumps with head scarps that are visible on air photos	Landslides sourced from non-competent formations
A1	Unconsolidated, poorly sorted alluvium	Alluvium in active channels

that are interpreted as deltaic beds (Link & Osborne, 1982). The diverse array of features in facies L1 implies that the small lake in Upper Ojai Valley was rapidly changing (McLane, 1995).

The areas where the valley floor is covered by alluvium and underlain by conglomeratic facies are planted with orange orchards (figure 16a). In contrast, the landscape in Upper Ojai Valley is smooth and dominated by grassy vegetation (figure 16b). Exposures of facies L1 are limited to ~2 km of Lion Creek in Upper Ojai Valley where the topography is very flat and no orchards are planted. Therefore, the lithofacies is interpreted to underlie most of Upper Ojai Valley (figure 15) and represents a lacustrine deposit rather than just ponded sediments representative of a shallow poorly drained area.

In addition, multiple intervals of similar fine-grained lacustrine deposits are interpreted based on water well logs within the basin fill of Ojai Valley (Kear, 2005). Although subsurface data is not available for Upper Ojai Valley, the presence of lakes in Ojai Valley suggests that lakes could have been more extensive and longer lived than the scarce exposures suggest in Upper Ojai Valley.

Facies LS1

The LS1 facies is composed of landslide and slump deposits. In the majority of the localities, a head scarp is usually present and lobate toes are less common. The mapped locations (figure 15) correspond with the locations of landslides on maps from previous workers (e.g. Dibblee, 1987a & b, 1990; Tan *et al.,* 2005a & b; Tan *et al.*, 2006). Landslides are common in the steeper topography composed of the non-competent formations described in table 1. Many of the deposits are in close proximity to active faults.

Facies A1

Facies A1 corresponds to the unconsolidated, poorly sorted, subrounded, fine sand to boulder size alluvium in active channels of the drainages shown in figure 4.

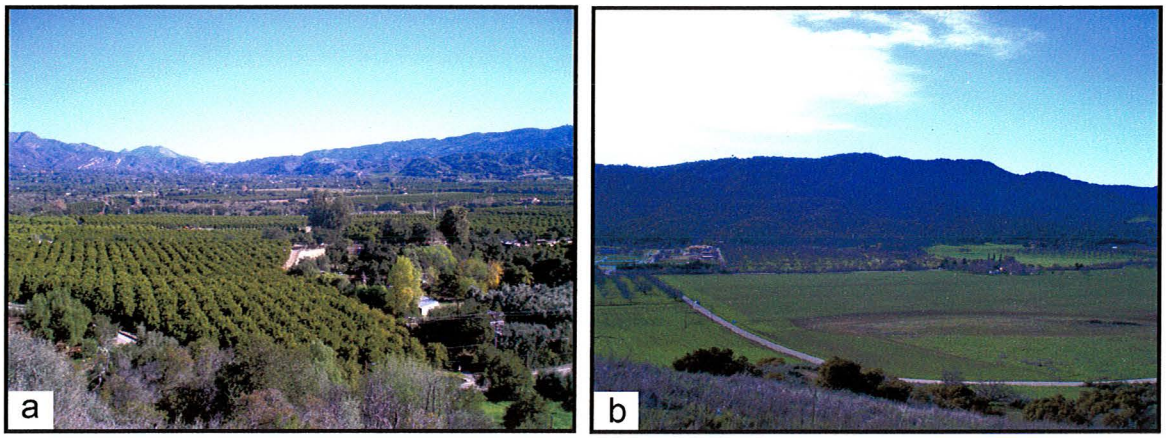

Figure 16. Photographs comparing the valley floors in Ojai and Upper Ojai valleys. (a) View looking to west across Ojai Valley. Note the extensive orchards planted throughout the valley. (b) View looking south across Upper Ojai Valley. Note the lack of orchards and the smooth surface.

3.3.2 Source

As evident by all of the clast counts (figure 7 & 8), the majority of the clasts in the sections measured in Lion Canyon are composed of competent grey, tan, buff, and brown-colored sandstones. The only in situ sandstones with similar characteristics include the Juncal, Matilija, Cozy Dell, and Coldwater Formations, exposed in the Topatopa and eastern Santa Ynez ranges to the north (table 1 & figure 5). South of the study area the bedrock consists of diatomaceous fine-grained sandstones, siltstones, and mudstones. Thus, the ranges to the north of the study area are the likely source for the clasts for the majority of the basin fill.

Red sandstone clasts make up >10% of the clasts within the basin fill (figures 7 & 8) The only red-colored sandstone within the study area is found within the Sespe Formation (table 1 & figure 5). Therefore, the clasts composed of red sandstone could be derived from the Sespe Formation, which underlies the fill in Ojai and Upper Ojai valleys (figure 5). In addition to red-colored sandstone, conglomerates with clasts of igneous and metamorphic origin are found within the Sespe Formation (table 1; Howard, 2005). The igneous and metamorphic clasts could be derived from the conglomeratic sections of the Sespe Formation.

The Monterey Formation is dominated by white-weathering diatomaceous shale-(angular clasts in figure 6d) and is exposed solely on Sulphur Mountain, located directly to the south of the Ojai and Upper Ojai valleys (figure 5). Any sandstone within the Monterey Formation is lighter in color and fine-grained compared to the sandstone clasts within the basin fill (table 1). The white shale clasts incorporated at the top of the basin fill exposed in Lion Canyon are in close proximity and identical to the Monterey Formation. Thus, Sulphur Mountain is the likely source for these clasts.

3.3.3 Paleocurrents

Rose diagrams 02 and 03 (figure 9), both located within the east bank of the Ventura River, show that imbricated clasts are oriented so that the paleodrainage flowed to the south. These orientations are nearly identical to the configuration of the modern Ventura River, suggesting that this drainage has been present since initial deposition in the basin.

On the other hand, imbricated clasts, shown by rose diagrams 04, 05, and 07 in the central part of the basin are oriented such that the paleodrainage flowed to the west (figure 9) even though the interpreted source of the basin fill is from the ranges to the north. Additionally, both Lion Creek and San Antonio Creek currently flow to the west. Both drainages are incising through the basin fill and do not have large enough flows to deposit such coarse-grained deposits. This suggests that the basin fill was deposited by a larger drainage system compared to the modern configuration. Rose diagram 06 (figure 9) shows the paleocurrent to the southwest and is likely displaced by one of the Oak View faults.

3.3.4 Summary of basin filling

In all exposures of the basal contact of the fill, the stratigraphically lowest, and therefore, oldest portion of the Quaternary basin fill is composed of facies C1 (e.g. figure 7-9 & 16). At these locations, clasts are almost entirely composed of competent sandstones derived from ranges in the north (figures 7 & 8), no clasts are composed of white shale, and orientation of imbricated clasts suggest that the paleodrainage flowed to the west (figure 9). Furthermore, in all areas, the base of the basin fill is in unconformable contact with Oligocene through middle Pleistocene-age strata that are more deformed than the fill itself (figure 7). These observations are evidence that initial deposition of basin fill occurred in the middle Pleistocene via alluvial fans and a braided fluvial system with material sourced from the uplift and subsequent erosion of the eastern Santa Ynez and Topatopa ranges. No white shale clasts of the Monterey Formation are present in the bottom of the basin fill. This implies that uplift of Sulphur Mountain had initiated because sediments were trapped and flow was channeled to the west but the Monterey Formation was not exposed on Sulphur Mountain. There is no evidence for deposition over Black Mountain, suggesting that depocenters in Ojai and Upper Ojai valleys have always been separate.

As uplift of Sulphur Mountain continued, the anticlinorium gained enough topographic relief to begin to contribute clasts to the basin, as evident by the clast counts that contain clasts composed of Monterey Formation near the top of the measured section in Lion Canyon (Figure 7). Additionally, sporadic clasts from the basin fill are perched on the footwall of the Lion fault on the north flank of Sulphur Mountain, which suggests that the basin fill or other Plio-Pleistocene sediments originally covered some of Sulphur Mountain and have since eroded away. This also explains the lack on Monterey clasts in the lower section because as uplift of Sulphur Mountain continued, an unknown thickness of conglomerate had to erode away before the Monterey Formation was even exposed. Average clast size also decreases from over 12 cm at the base to less than 7 cm and the top of the section in Lion Canyon (table 3) because reworking of sandstone clasts eroded from Sulphur Mountain reduced the grain size.

The uppermost basin fill in Upper Ojai Valley is composed of lacustrine deposits with radiocarbon dates ranging in age from ~15 to over 46 ka. Landslides bound the westernmost portion of Upper Ojai Valley (figure 15). These landslides and ponding behind the actively uplifting Sulphur Mountain blocked the drainage outlet for the basin and led to the formation of a late Pleistocene age lake in Upper Ojai Valley.

There is a lack of subsurface data in Upper Ojai Valley. Only the upper ~ 5 m of basin fill is exposed so the actual thickness of the lacustrine deposits is unknown and the existence of a lake prior to ~46 ka is undeterminable. Clay-rich layers, interpreted from water well logs throughout the basin fill in Ojai Valley, impede flow in the groundwater aquifer and are interpreted as lacustrine deposits (Kear, 2005). This is evidence that intermittent lakes have formed throughout the late Pleistocene in both Ojai and Upper Ojai valleys and only the uppermost lacustrine deposits are exposed.

The presence of debris flows in facies L1 and radiocarbon results suggest that the rate of basin filling in Upper Ojai Valley is highly variable. The radiocarbon samples are separated by ~ 0.75 m and the samples are ~ 31 ka apart. These data imply an average sedimentation rate of ~ 0.024 mm/yr. However, a major bedding contact, which may be an unconformity, is present between the samples (figure 6f), which represents an unknown amount of time. Therefore, the sedimentation rate was not constant throughout the late Pleistocene.

4. TECTONICS

North-south shortening across the Ojai valleys is dominated by sub-parallel faults and folds. To the west of Ojai Valley, movement on the north-dipping Red Mountain fault and associated folding accommodates all of the south-vergent shortening (Huftile, 1991; figure 2) and becomes a blind thrust beneath Ojai Valley (Huftile and Yeats, 1995). East of Santa Paula Creek, the north-dipping San Cayetano fault accounts for most of the horizontal shortening in the region (Huftile, 1991). The San Cayetano fault reaches the surface along the north edge of Upper Ojai Valley (figure 5). The fault turns into a blind thrust within the Sespe Formation at the eastern end of Ojai Valley and continues beneath the Topatopa Mountains (figure 5; Huftile & Yeats, 1995). The south-dipping Big Canyon, Sisar and Lion faults, here called the Lion fault system, is a back thrust that accommodates a portion of the convergence south of the Ojai valleys. Therefore, the Ojai valleys represent a transition zone where shortening is transferred from the San Cayetano fault, to the Lion fault system, and then to the Red Mountain fault (Huftile, 1991; figure 3).

In addition to the structural complexity, many of the faults in the study area, as well as the rest of the wTR, are bedding-parallel at the surface but displace strata at an angle at depth. Thus, quantification of slip is difficult to determine due to lack of piercing points both laterally and vertically based on surficial observations. Some faults displace Quaternary age surfaces and sediments, which allows for observation of displacement (Rockwell, 1988; Rockwell *et al.*, 1984; Yeats, 1981). The three-dimensional geometry of the basin fill displayed in figures 11 and 15 allows interpretation of the amount of vertical separation on the basin bounding faults. These estimates, divided by vertical slip rates calculated by previous workers, can be used to constrain the age of the basin bounding faults. The basin fill is cut by these faults, so the basin fill is older than the faults. Therefore, the ages of the basin bounding faults represent the minimum ages for initial deposition.

4.1 Data, observations & calculations

4.1.1 Black Mountain & the Arroyo Parida-Santa Ana fault

In Ojai Valley, just east of the Ventura River, the Arroyo Parida-Santa Ana fault displaces Oak View terrace Qt6a and has a vertical separation of 14 ± 0.3 m (Rockwell *et al.*, 1984). The terrace surface is dated at 41,408 ± 1,233 years from soil chronology, calibrated radiocarbon, and ^{10}Be cosmogenic exposure dating methods (Rockwell et al., 1984; DeVecchio *et al.*, in press). This age and vertical separation equates to vertical slip rate of ~ 0.34 ± 0.02 mm/yr for the Arroyo Parida-Santa Ana fault at this location.

The base of the fill is exposed at an elevation of ~195 m in San Antonio Creek just south of the Arroyo Parida-Santa Ana fault (figure 15). The best-constrained thickness of basin fill to the north of the fault is 150 m (figure 11). The elevation of the surface of Ojai Valley in this area is ~255 m so the elevation of the basal contact is ~ 105 m above sea level. Therefore, assuming a planar contact, the maximum vertical separation on the Arroyo Parida-Santa Ana fault is approximately 90 m. Assuming a constant slip rate of ~ 0.34 ± 0.02 mm/yr (Rockwell *et al.*, 1984) and that all of the

displacement on the fault has occurred since initial deposition, then the fault has been active for the last 265 ± 15 ka.

4.1.2 The San Cayetano fault

The San Cayetano fault has a stratigraphic separation of 2.6 km in Upper Ojai Valley between the Sespe and Vaqueros Formations (Huftile 1991). Assuming a constant slip rate of 1.35 ± 0.4 mm/year since the late Pleistocene, the San Cayetano fault has been active for ~1.9 Ma (Rockwell, 1988).

The vertical slip rate for the San Cayetano fault at Sisar Creek is 0.75 ± 0.15 mm/year based on soil development of a 15-20 ka fan surface displaced by the fault (Rockwell, 1988). The San Cayetano fault juxtaposes basin fill against the Sespe Formation in Upper Ojai Valley and the vertical separation of the base of the basin fill on either side of the fault is approximately 300 m (figures 10 & 11). Based on the above slip rate and vertical separation, the San Cayetano fault initially displaced the base of the fill at 415 ± 85 ka. This is a minimum age because the fill could have been deposited and then subsequently been cut by the fault.

4.1.3 Sulphur Mountain & the Lion fault system

The basin fill on the south side of Upper Ojai Valley, adjacent to the Lion fault, is at least 200 meters thick (figures 10 & 11). Assuming the fill deposition initiated prior to 415 ± 85 ka in Upper Ojai Valley, the average vertical slip rate on the Lion fault for the mid- to late Pleistocene is 0.64 ± 0.24 mm/yr.

Near the base of Lion Canyon, the Lion fault also displaces the Miocene Rincon Formation over approximately 60 m of basin fill (Figure 17). The three-dimensional wedge-shaped geometry of the fill in Lion Canyon (figures 11 & 17) suggests that the fill was deposited into a paleovalley by a fluvial system (facies C1, figure 15) that flowed to the west (figure 9) from Upper Ojai Valley. The fill was likely never as thick at this location as in the eastern portion of Upper Ojai Valley and not preserved due to uplift on the Oak View and Lion faults.

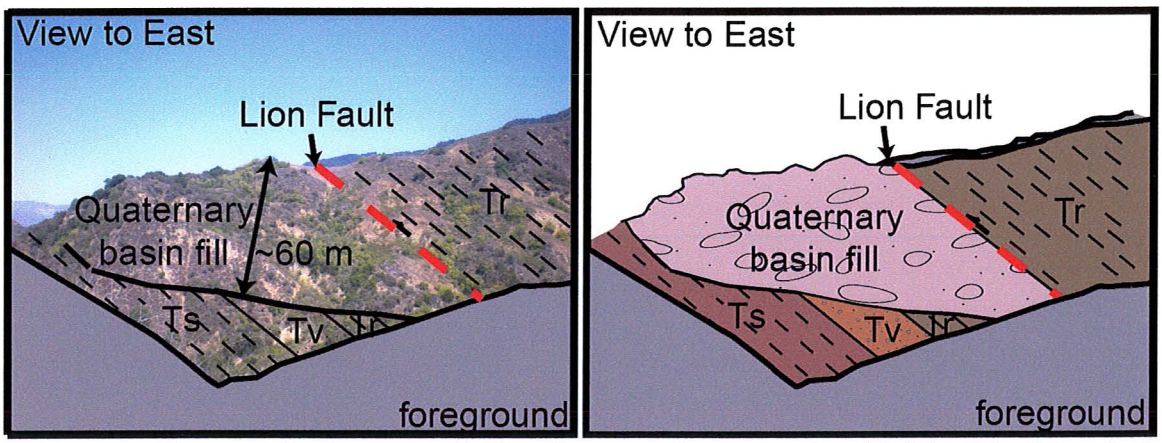

Figure 17. Photograph of outcrop (left) and cartoon interpretation (right) of the Lion fault in Lion Canyon that displaces up to 60 m of Quaternary basin fill below the Rincon Formation.

Assuming the base of the basin fill in Lion Canyon is time-correlative to the base in Upper Ojai Valley, the base of the fill is at least 415 ± 85 ka. Therefore, the minimum vertical uplift rate on the Lion fault within Lion Canyon is 0.15 ± 0.03 mm/yr because an unknown amount of fill has been eroded from both the hanging wall and footwall.

4.1.4 Longitudinal stream profile of Lion Creek

Lion Creek flows westward from near the center of Upper Ojai Valley, through Lion Canyon, and then joins San Antonio Creek (figure 18a). A longitudinal profile of Lion Creek was extracted from a 3-meter digital elevation model using ArcGIS (figure 18 b). In figure 18b, the thickness and elevation of facies C1 are superimposed onto the stream profile to display the relationship between the modern and ancient drainages.

On figure 18, point A represents the headwaters and has an elevation of 470 m. Point B is located at the top of Lion Canyon and has an elevation of 375 m. The gradient from point A to B, through Upper Ojai Valley, is 13.5 m/km. From point B to C, Lion Creek flows parallel to Black Mountain, and point C is located at the end of Black Mountain at an elevation of 170 m. From point B to C, where Lion Creek flows parallel to Black Mountain, the gradient is significantly steeper at 23.8 m/km. In this segment, Lion Canyon is a slot canyon with a width as little as several meters and a depth up to 40 m that is incised into a meandering pattern. Point D is the base of Lion Creek and Lion Canyon and the gradient from point C to D 9.80 m/km. These changes in stream gradient are discussed below.

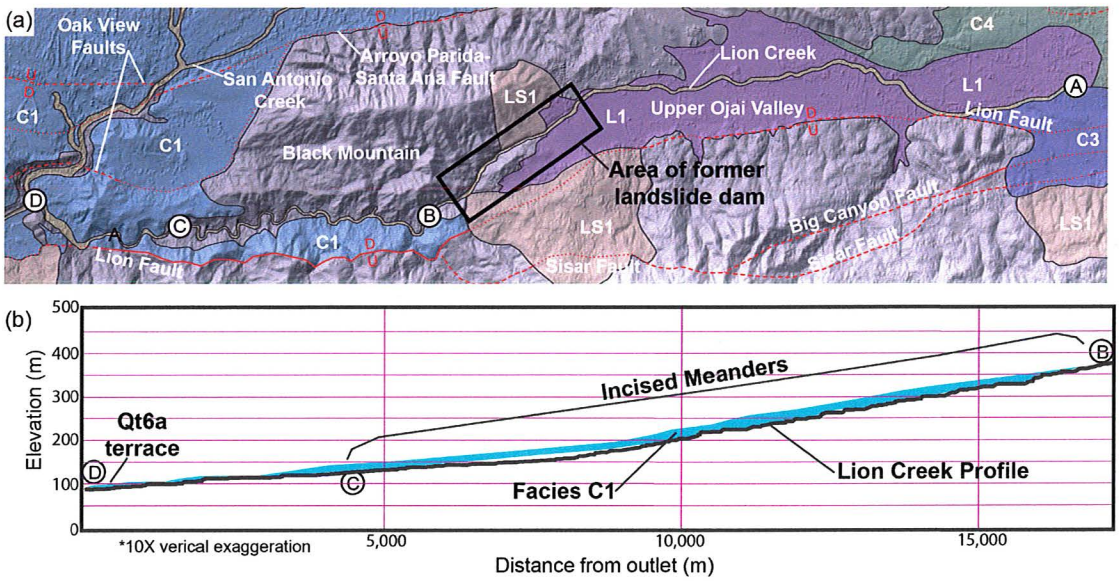

Figure 18. Map and longitudinal profile of Lion Creek. (a) Colors on map represent lithofacies discussed in text (figure 15, tables 2 & 6). (b) Longitudinal stream profile of Lion Creek from point B to D and locations of facies C1 outcrops in Lion Canyon.

4.2 Results & interpretations

4.2.1 Formation of depocenters

The basin fill reaches a maximum thickness of 240 m in the southeastern part of Ojai Valley (figure 11). This depocenter is located in the footwall of the Arroyo Parida-Santa Ana and San Cayetano faults. Due to the location of this depocenter being in such close proximity to two active faults, the formation of this depocenter is likely tectonically controlled.

The Ojai Valley basin is bounded to the south by Black Mountain, which is composed of Lion Mountain anticline and Reeves syncline (figure 5). All of the basin fill lies in angular unconformity with the Black Mountain structures (figure 7; Huftile, 1991 & Kear, 2005), implying uplift and erosion of the area prior to deposition. The folds are also cut by the Arroyo Parida-Santa Ana fault (figure 3) suggesting that the fault is younger. Therefore, the location of the depocenter in Ojai Valley is due to movement on the Arroyo Parida-Santa Ana fault, which propagated to the surface at least 265 ± 15 ka (table 7) but prior to this time, folding of Lion Mountain anticline and Reeves syncline may have created a topographic feature that trapped sediments and diverted drainages to the west.

Table 7. Summary of displacements and slip rates on basin-bounding faults in Ojai and Upper Ojai valleys. *Calculations in this study are *italicized* and references are listed below.

Fault name	Vertical separation	Vertical slip rate	Age of structure
Arroyo Parida-Santa Ana fault	*90 m*	*0.34 ± 0.02 mm/yr*	*265 ± 15 ka*
San Cayetano fault	2.6 km [D]	1.35 ± 0.4 mm/yr [C]	1.9 Ma [C]
Lion Fault	60-200 m	*0.37 ± 0.25 mm/yr*	*415 ± 85 ka*

* [A] Rockwell, 1983; [B] Rockwell *et al.*, 1984; [C] Rockwell, 1988; [D] Huftile, 1991

Table 8. Calculated ages of the basin fill and associated sedimentation rates in Ojai and Upper Ojai valleys. *Calculations in this study are *italicized* and references are listed below. **Based on the fact that the base of the fill must pre-date faulting.

Location	Max. basin fill thickness	Min. age of base of basin fill**	Age of top of basin fill	Sedimentation rate
Ojai Valley	*240 m*	*243 ± 13 ka*	15-30 ka [B & C]	1.02 ± *0.18 mm/yr*
Upper Ojai Valley	500 m [D]	*415 ± 85 ka*	*< 15 ka*	*1.31 ± 0.28 mm/yr*
Lion Canyon	*60 m*	*415 ± 85 ka*	15-30 ka [B & C]	*0.16 ± 0.04 mm/yr*

* [A] Rockwell, 1983; [B] Rockwell *et al.*, 1984; [C] Rockwell, 1988; [D] Huftile, 1991

Similar to the depocenter in Ojai Valley, the 500 m deep depocenter in Upper Ojai Valley (figure 11) is bounded by two faults. The depocenter is located in the footwall of the San Cayetano and Lion faults and is, therefore, likely tectonically

controlled. Based on the amount vertical separation and slip rate on the San Cayetano fault, the depocenter in Upper Ojai Valley is at least 415 ± 85 ka (table 7).

Slip rates on the San Cayetano fault are well defined (Rockwell, 1988) and can be used to interpret the age of depocenter in Upper Ojai Valley. Assuming the fill was initially deposited behind Sulphur Mountain, which uplifted most recently along the Lion fault (Huftile, 1991), slip rates for the Lion fault can be inferred (table 8) based on the age of this depocenter.

4.2.2 Style of convergence & preservation of the basin fill in Ojai & Upper Ojai valleys

Point C (figure 18), located near the base of Lion Canyon and at the westernmost part of Black Mountain, represents the boundary between two dramatically different structural zones. Point C is approximately along strike with the Red Mountain fault (figure 2), the easternmost edge of terraces formed by the Ventura River (figure 4), and the region of extremely thin basin fill to the north of the Arroyo Parida-Santa Ana Fault in the center of Ojai Valley (figure 11). To the west of point C, convergence is accommodated on numerous shallow flexural slip faults in the hanging wall of the Red Mountain fault/blind thrust (the Oak View faults). The Quaternary basin is > 6 km wide and the basin fill ranges from 40-120 m in thickness (figure 11). This thickness is a result of uplift accommodated over a wide area as well as erosion of the basin fill along the Ventura River. On the other hand, in the regions to the west of point C, only the San Cayetano, Arroyo Parida-Santa Ana, and Lion faults accommodate convergence. The Upper Ojai Valley basin is less than 3km wide and greater than 200-500 m deep. Also, Black and Sulphur mountains are uplifted to the west of point C.

5. DISCUSSION

5.1 Tectonic versus climatic influences on basin filling

A complex relationship exists between rock uplift and climate throughout the development of an intramontane basin. Rates of faulting vary within the basin and throughout Quaternary time implying that tectonics should control local deposition. In the case that climatic fluctuations are the control on these processes, the timing of deposition and erosion throughout an entire region should be synchronous.

The Ojai and Upper Ojai basins are both located in the footwalls of active faults and the deepest parts of the basins are not in the center of the valleys (figure 11). Instead, both basins are asymmetric and depocenters are located in the eastern portion of each valley where the basin bounding faults are closest to each other and subsidence may be highest (figure 11). Moreover, calculations of the age of basin bounding faults suggest that the Upper Ojai Valley could be older than Ojai Valley. These data are evidence that the main control on formation of the basins and the locations of the depocenters is tectonics.

In the Ojai valleys, a wetter climate with higher rates of precipitation would increase erosion rates in the ranges and therefore, increase the sediment supply. More precipitation would result in a higher energy depositional environment that is capable of transporting boulder size clasts present in facies C1 (figure 6a & b; table 2). Also, the Pleistocene climate in the northern hemisphere is known to be cooler and more strongly variable than the time periods before and after (Mudelsee & Schulz, 1997; Zachos et al., 2001; Lisiecki & Raymo, 2007). Therefore, although the accommodation space in the Ojai and Upper Ojai basins was created due to tectonic subsidence, basin filling could have been influenced by smaller scale climatic perturbations that cannot be constrained based on the data presented in this study.

Sedimentologic observations and radiocarbon dating of the uppermost basin fill in Upper Ojai Valley (facies L1, figure 15) suggest the existence of a late Pleistocene age lake in Upper Ojai Valley that formed upstream from a landslide dam. Multiple studies of landslide-dammed lakes throughout the world suggest that both tectonics and climate play a role in the formation and failure of these lakes formed in mountainous terrain (*e.g.* Fillion *et al.*, 1991; Trauth & Strecker, 1999; Trauth *et al.*, 2003; Korup, 2004; Dai *et al.*, 2005; Korup & Tweed, 2007; Pratt-Sitaula *et al.*, 2007). In these studies, landslides are commonly triggered by increased precipitation or earthquake events.

An increase in precipitation due to a different climate could be source of the excess water in Upper Ojai Valley that formed a lake. Additionally, a more humid climate could have triggered landslides that bound the valley (*e.g.* Trauth & Strecker, 1999; Trauth *et al.*, 2003). The landslides are, however, covering the trace of the Lion fault in Upper Ojai Valley (figure 15) and the western Transverse Ranges are one of the most tectonically active regions in the world (Nicholson, *et al.*, 2007), suggesting that an earthquake could have triggered failure. Therefore, due to the lack of ages on landslides in Upper Ojai Valley and no paleoseismic record for the Lion fault, it is undeterminable at this time to determine if the landslides that formed the dam were triggered by tectonics or by increased precipitation in a more humid climate.

5.2 Late Pleistocene incision & erosion

5.2.1 Partitioning of drainages in Upper Ojai Valley

Sisar Creek turns abruptly to the east in Upper Ojai Valley in close proximity to the headwaters of Lion Creek (figure 4) and in the eastern part of Upper Ojai Valley, Sisar Creek is incising into the bedrock. The incision suggests that the drainage system is responding to a change, perhaps because Sisar Creek used to flow to the west and drain Upper Ojai Valley. According to Capuzzo & Wetzel (2004), large scale tilting induces headward erosion of valleys and capture of rivers draining in the opposite direction. This may be the situation in Upper Ojai Valley, where uplift associated with Black Mountain to the west combined with headward erosion in Santa Paula Creek led to the capture of Sisar Creek.

Santa Paula Canyon is filled with fluvial conglomerates interpreted as late Pleistocene fill (facies C2, figure 15, table 2). Due to the capture of Sisar Creek in Upper Ojai Valley, the amount of flow, sediment supply, and drainage basin area of Santa Paula Creek changed rapidly. The series of terraces in Santa Paula Canyon (figure 6c) could have formed as the fluvial system adjusted to these changes.

5.2.2 History of Lion Canyon

A lake was present at the top of Lion Canyon, in western Upper Ojai Valley from at least 15 to 46 ka (figure 18). At the bottom of Lion Canyon is a Q6a (~38 ka) age terrace that has been incised by Lion Creek (figures 12 & 18; Rockwell et al., 1984). Lion Canyon is located between these two surfaces and it is filled with facies C1 (figures 15, 17 & 18) This configuration suggests that a continuous Valley with a fluvial system that flowed west was present from Upper Ojai Valley to Oak View at Q6a time.

Lion Creek has incised Lion Canyon into a meandering pattern between points B and D on figure 18a. The meandering pattern suggests that prior to incision the previous drainage system had a low gradient (Holm, 2003; Matmon *et al.*, 2009). Incised meanders form when the stream gradient increases as a result of tectonics or a change in base level and the meandering stream pattern is superimposed (Holm, 2003). The entire area to the south of the Arroyo Parida-Santa Ana fault has uplifted since the formation of the Oak View terraces (Rockwell *et al.*, 1984). These observations suggest that uplift initiated the incision of the meanders in Lion Canyon as well as incision by Santa Paula Creek and the Ventura River.

In addition to incision in Lion Canyon in response to uplift of the area south of the Arroyo Parida-Santa Ana fault, a landslide dam may have been present at the top of Lion Canyon from ~ 15 to greater that 46 ka. Incision commonly occurs at the downstream end of a landslide dam due to the instantaneous change in stream gradient and decrease in sediment supply (Pratt-Sitaula *et al.*, 2007). Therefore, the landslide dam could have contributed to the incision of Lion Canyon.

Presently, Lion Creek flows through Upper Ojai Valley, through the former landslide dam, and down Lion Canyon (figure 18). The lacustrine deposits are as young as ~ 15 ka, suggesting that the outlet at the west end of Upper Ojai Valley was blocked until this time. Headward erosion on the Lion Canyon side of the dam likely triggered dam failure. This failure, however, was gradual because catastrophic floods due to

landslide dam failure are known to produce catastrophic valley-floor aggradation, active-channel widening, and downstream dispersion of sediment, during which little bedrock erosion seems to be achieved. (Dai *et al.*, 2005; Korup & Tweed, 2007). Therefore, the incised meanders in Lion Canyon could have been destroyed if the dam failed catastrophically and no flood deposits are present.

The longitudinal profile along Lion Creek not only reflects the drainage evolution of Lion Creek, but also the transition in structural styles of the Lion fault system because Lion Creek flows nearly parallel to the structural grain of the area. Overall, the elevation change of nearly 400 m from A to D on figure 18 is due to broadening of the zone of deformation and decreased uplift to the west. The profile from points A to B shows the rapid facies change from facies C4 to L1 combined with a 0.2 mm/yr incision since 15 ka. Point B to C is a rapidly incising slot canyon that is nearly parallel to the Lion fault and is a nick-point reflecting the adjustment of the drainage system. The profile from C to D reflects the deformational style of the Red Mountain fault with broad, flat deformation and terraces of the Ventura River.

5.2 Geologic evolution of Ojai and Upper Ojai valleys

5.2.1 Late Pliocene to Middle Pleistocene

Based on work by Rockwell (1988), slip on the San Cayetano fault initiated at 1.9 Ma, which led to the uplift of the eastern Santa Ynez and Topatopa Mountains. Material that eroded from this uplifted area throughout this time was either transported through the Ojai area because there were no structures present to trap the sediments or deposited and then subsequently eroded before uplift of Black and Sulphur mountains (figure 19a).

Folding of the Lion Mountain anticline and Reeves syncline occurred within the footwall of the San Cayetano fault and ceased prior to any deposition of Pleistocene basin fill (Huftile, 1991). Prior to 1.2 Ma and as deformation propagated to the south, folding of Big Canyon syncline and Sulphur Mountain anticlinorium started (Huftile, 1991) (figure 19b). Although this folding likely produced topographic relief in the area, all of these structures as well as any deposited sediment were highly eroded, as evident by the angular unconformity that is always present at the base of the basin fill that is currently preserved in the Ojai area (*e.g.* figures 5, 7 & 17).

5.2.2 Middle to Late Pleistocene (basin formation and filling)

Based on the assumption that the locations of depocenters in Ojai and Upper Ojai valleys are tectonically controlled because they are located in the footwalls of basin bounding faults (figure 11), the minimum age of basin formation corresponds to the age of the initial slip on the basin bounding faults (table 7). These are minimum ages because the folds that form Black and Sulphur mountains, Lion Mountain anticline and Sulphur Mountain anticlinorium, respectively, are older than the faults that bound the basins because the faults cut through the folds (figure 3). The folds, however, could have trapped sediments before the faults propagated to the surface (figure 19c). From this, the basin in Ojai Valley formed more than 265 ± 15 ka based on the age of the Arroyo Parida-Santa Ana fault. Likewise, the basin in Upper Ojai Valley is greater than 415 ± 85 ka (figure 19d).

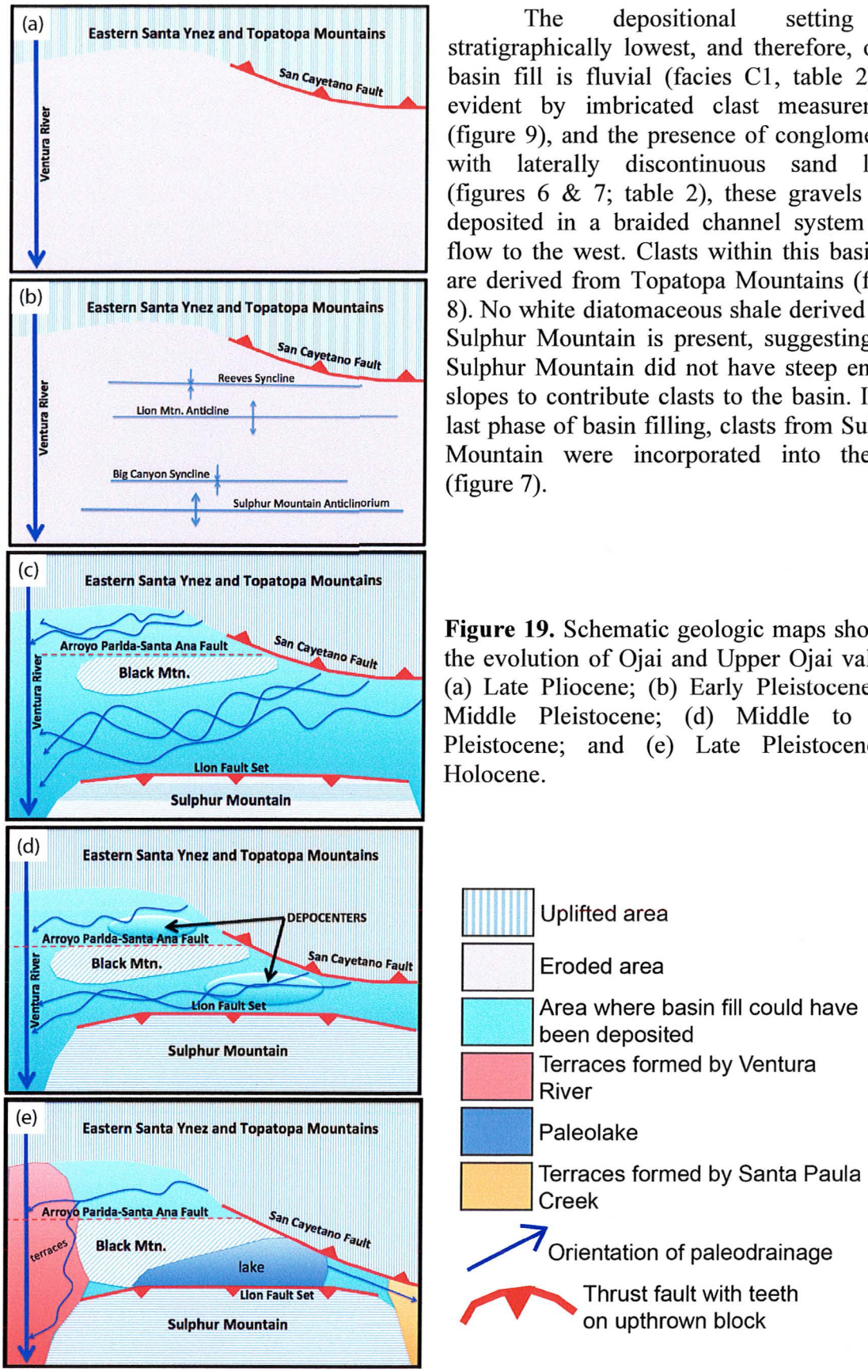

The depositional setting of stratigraphically lowest, and therefore, oldest basin fill is fluvial (facies C1, table 2). As evident by imbricated clast measurements (figure 9), and the presence of conglomerates with laterally discontinuous sand layers (figures 6 & 7; table 2), these gravels were deposited in a braided channel system with flow to the west. Clasts within this basin fill are derived from Topatopa Mountains (figure 8). No white diatomaceous shale derived from Sulphur Mountain is present, suggesting that Sulphur Mountain did not have steep enough slopes to contribute clasts to the basin. In the last phase of basin filling, clasts from Sulphur Mountain were incorporated into the fill (figure 7).

Figure 19. Schematic geologic maps showing the evolution of Ojai and Upper Ojai valleys. (a) Late Pliocene; (b) Early Pleistocene; (c) Middle Pleistocene; (d) Middle to Late Pleistocene; and (e) Late Pleistocene to Holocene.

5.2.3 Late Pleistocene to Holocene (terrace formation and drainage partitioning)

Paleocurrent data suggests that a major drainage with flow to the west has been present since initial deposition of basin fill (figures 9 & 19c). The entire drainage system flowed to the west until the formation of a landslide dam in the westernmost part of Upper Ojai Valley (figure 15). The landslides could have formed a dam that blocked the outlet for the basin and led to the formation of a lake in Upper Ojai Valley that was bounded by landslides to the west, Black Mountain to the northwest, the Topatopa Mountains to the northeast and Sulphur Mountain to the south (figure 19e). Radiocarbon dating of (section3.2.4) organic rich fine-grained sediments (facies L1, table 2; figure 6f) in the uppermost basin fill in Upper Ojai Valley and upstream from the dam suggests this lake was present from ~15 to over 46 ka.

Incision has occurred on all drainages since the abandonment of the oldest preserved terraces (maximum of 105 ka, Rockwell *et al.* 1984). Lion Creek has incised Lion Canyon into entrenched meanders in the time since the landslide dam formed (46 ka?). Headward erosion of Lion Canyon incised through the landslide dam less than 15 ka based on the age of the youngest lacustrine deposits in Upper Ojai Valley.

5.2.4. The future of Ojai and Upper Ojai valleys

If the Lion Fault has an uplift rate of 1.1 mm/yr (Rockwell *et al.*, 1984), then the horizontal slip rate for a fault dipping 60° is 0.64 mm/yr. The horizontal component of slip for the San Cayetano fault, which dips 50° and has a vertical rate of 0.75 mm/yr is 0.63 mm/yr. Upper Ojai Valley is 1.25 km wide, so at this rate, the valley will begin to converge upon itself in less than 100 ka. Eventually, the same thing will happen to the eastern portion of Ojai Valley.

At the western end of the intramontane basin, the Ventura River is incising at a rate of ~ 0.5 to 1.3 mm/yr (Rockwell *et al.*, 1984). If the rate of erosion is similar to the uplift rate, then all of the uplifted basin fill will erode within 240 ka. This, combined with zipping up of the basin from the east, and transfer of slip to other structures, will destroy the Ojai valleys.

The basin fill in Ojai and Upper Ojai valleys is important because intramontane basins are often poorly preserved and quickly destroyed. Also, they serve as ideal groundwater and oil reservoirs. The exposures in the area allow for the study of how the basins were formed and information on how they are being destroyed. For example, at Silverthread oil field, located just to the east of Santa Paula Creek, a wedge of Quaternary conglomerate, interpreted to be the Saugus Formation located in the subsurface within the footwall of the San Cayetano fault (Rockwell, 1988). This wedge of sediment is a preserved intramontane basin but direct observation of the sediments is not possible because they are not at the surface. To the east of Ojai Valley, no intramontane basin sediments are preserved. If the Pleistocene basin continued to the east of the Ventura River, it has now completely eroded away. This furthermore verifies that the Ojai valleys provide a rare and unique glimpse at Pleistocene intramontane basin formation and erosion.

5.3 What is the basin fill in Ojai and Upper Ojai valleys?

Previous workers have interpreted the conglomerates in Ojai to be several m thick terrace gravels (*e.g.* Rockwell *et al.*, 1984). This study verifies that the Ojai conglomerates are much thicker (up to 500 m, figure 11), more consolidated (figure 12), and more laterally extensive (figure 15) than lag deposits found on terrace treads.

Other workers have interpreted the basin fill in Ojai and Upper Ojai valleys as Saugus Formation (*e.g.* Rockwell et al., 1988; Yeats et al., 1988; Huftile, 1991; Huftile and Yeats, 1995). Although the age of initial deposition in Ojai and Upper Ojai valleys may be correspond with the age of Saugus Formation to the south (0.2-0.63 Ma), there is no evidence that the conglomerates in the Ojai valleys ever covered the crest of Sulphur Mountain and cannot be correlated to the Saugus Formation. Additionally, the basin fill in Ojai and Upper Ojai Valley is still being deposited today via active alluvial fans sourced from both the Topatopa Mountains and Sulphur Mountain, which is not the Saugus Formation.

Alternatively, the basin fill in Ojai and Upper Ojai valleys represents fluvial gravels deposited by a paleodrainage system that flowed to the west. Remnants of this large paleodrainage system are still visible today (figure 20). Incision in Santa Paula

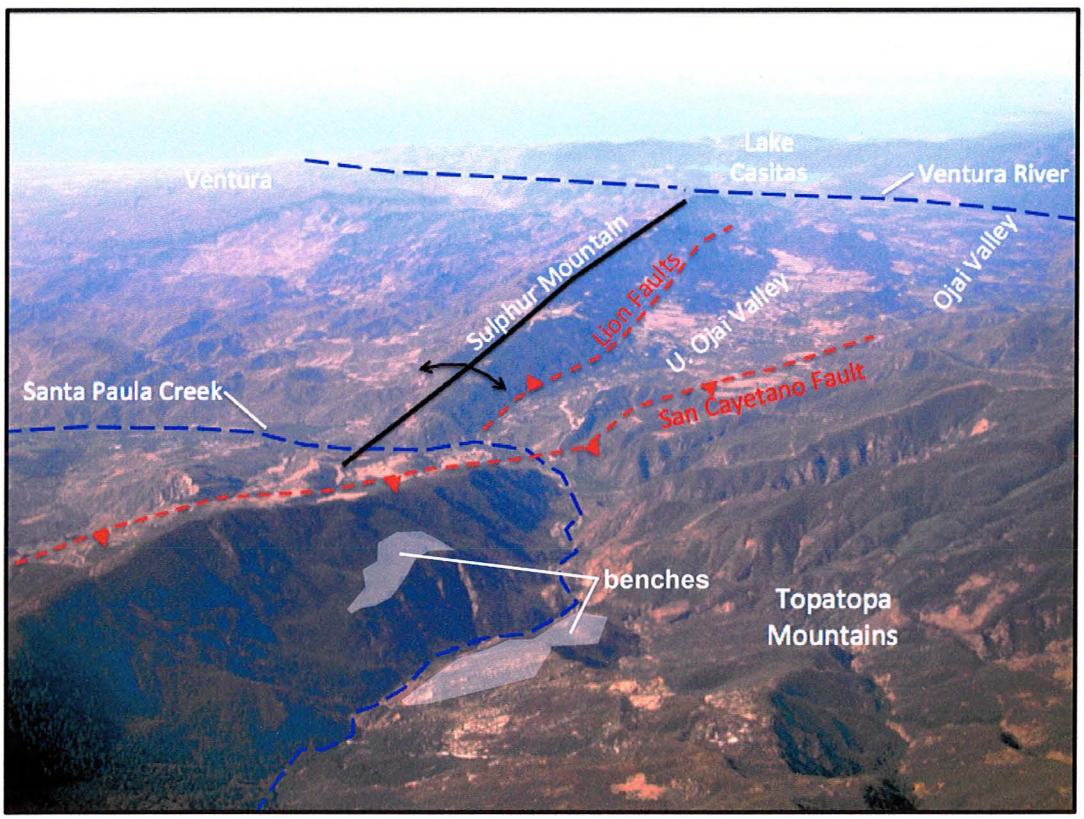

Figure 20. Annotated aerial view of the Ojai and Upper Ojai valleys looking southwest toward the Pacific Ocean and the city of Ventura. Modern drainages, locations of faults, and features that are remnant from a paleodrainage system are labeled.

Creek is steep and suggests that it has recently occurred but benches, that could have been part of the paleodrainage system, are perched on either side of the canyon. The Ojai and Upper Ojai valleys are flat surfaces that are dissected by Sulphur and Black mountains and the Lion and San Cayetano faults. All of these features are evidence that a paleodrainage system used to flow down Santa Paula Creek, across the Ojai valleys, and into the Ventura River (figure 20).

Located to the south of the Ojai area, the Santa Clara River system flows through a broad, flat-bottomed valley (figure 21). The valley is bounded by South Mountain and the Oak Ridge fault to the south and the southern flank of Sulphur Mountain to the north. The drainage system is braided and is a modern example of what the paleodrainage system in Ojai and Upper Ojai valleys could have looked like.

Figure 21. Annotated aerial view of the Santa Clara River, looking southwest toward the Pacific Ocean and the city of Ventura.

6. CONCLUSIONS

Consolidation of subsurface water- and oil-well data with slip rates from previous workers allows clarification of the process and timing of intramontane basin formation in Ojai and Upper Ojai valleys. Depocenters in Ojai and Upper Ojai valleys, now 240 and 500 m deep, respectively, initially formed behind uplifted folds in middle Pleistocene time. The folds were subsequently cut and further uplifted by basin bounding faults. In Ojai Valley, the Arroyo Parida-Santa Ana has uplifted Black Mountain and dissected the basin fill since at least 265 ± 15 ka. Likewise, the Lion fault system has uplifted Sulphur Mountain and dissected the basin fill in Upper Ojai Valley since at least 415 ± 85 ka. Both basins are asymmetric and located in the footwalls of basin bounding faults, so tectonics was the main control on basin filling.

Sedimentologic and stratigraphic description of all exposures of the basin fill in the Ojai valleys elucidates the processes of basin filling. In particular, clast counts and paleocurrent data suggest the oldest basin fill was deposited via a fluvial system that drained to the west and material was derived from the Topatopa Mountains, located northeast of the study area. Clasts derived from the Monterey Formation, which is exposed on Sulphur Mountain to the south of the valleys, do not appear in the basin fill until the upper 20 m. Unfortunately, $^{26}Al/^{10}Be$ cosmogenic burial dating was not successful so the basal age of the basin fill is not constrained. The uppermost basin fill in Upper Ojai Valley, however, is comprised of lacustrine deposits that range in age from ~15 to > 46 ka based on radiocarbon dating.

The relationship between the basin fill, active faults, fluvial terraces, and actively incising drainages are interpreted to reveal the Pleistocene landscape evolution in the area. For example, preserved terraces, lacustrine deposits, and exposures of basin fill suggest that a continuous valley was present from Upper Ojai Valley to the Oak View area and was filled with fluvial gravels. Subsequently, emplacement of a landslide dam and uplift of the area to the south of the Arroyo Parida-Santa Ana fault caused incision of all the drainages in Ojai Valley. In particular, Lion Creek formed incised meanders in Lion Canyon. Lastly, large-scale tilting in Upper Ojai Valley caused headward erosion in Santa Paula Creek that led to the capture of Sisar Creek, which diverted the flow to the east rather than the west.

REFERENCES

Allen, M., Jackson, J., and Walker, R., 2004, Late Cenozoic reorganization of the Arabia-Eurasia collision and the comparison of short-term and long-term rates, Tectonics, vol. 24, doi:10.1029/2003TC001530.

Atwater, T., 1998, Plate Tectonic History of Southern California with emphasis on the geology on the Western Transverse Ranges and Santa Rosa Island, *in* Weigand, P. W., ed., Contributions to the geology of the Northern Channel Islands, Southern California: American Association of Petroleum Geologists, Pacific Section, MP 45, p. 1-8.

Balco, G., J.O.H. Stone, & J.A. Mason, 2005, Numerical ages for Plio-Pleistocene glacial sediment sequences by 26Al/10Be dating of quartz in buried paleosols, Earth and Planetary Science Letters, vol. 232, p. 179-191.

Blair, T.C. & J.G. McPherson, 1994, Alluvial fan processes and forms, *in* Abrahams, A.D. & A.J. Parsons (eds.), Geomorphology of desert environments: Chapman and Hall, London, p. 354-402.

Boggs, S., 2006, Principles of Sedimentology and Stratigraphy, fourth edition: Pearson Prentice Hall, Upper Saddle River, 662 p.

Bronk Ramsey, C., 2010, Bayesian analysis of radiocarbon dates, Radiocarbon, vol. 51, no. 1, p. 337-360.

Brookfield, M.E., 1980, Permian intermontane basin sedimentation in southern Scotland, Sedimentary Geology, Vol. 27, n. 3, p. 167-175, 177-194.

Burbank, D.W. & Johnson, G.D., 1983. The late Cenozoic chronologic and stratigraphic development of the Kashmir intermontane basin, Northwestern Himalaya, Palaeogeography, Palaeoclimatology, Palaeoecology, v. 43, n. 3-4, p. 205-235.

Capuzzo, N. & A. Wetzel, 2004, Facies and basin architecture of the Late Carboniferous Salvan-Dorenaz continental basin (Western Alps, Switzerland/France), Sedimentology, vol. 51, p. 675-697.

Clark, P.U., D. Archer, D. Pollard, J.D. Blum, J.A. Rial, V. Brovkin, A.C. Mix, N.G. Pisias, & M. Roy, 2006, The middle Pleistocene transition: characteristics, mechanisms, and implications for long-term changes in atmospheric pCO2, Quaternary Science Reviews, vol. 25, p. 3150-3184.

Crouch, J.K. and J. Suppe, 1993, Late Cenozoic tectonic evolution of the Los Angeles basin and inner California borderland: A model for core complex-like crustal extension, GSA Bulletin, v. 105, no. 11, p. 1415-1434.

Crowell, J. C., 1974, Origin of the late Cenozoic Basins of southern California: Society of Economic Paleontologists and Mineralogists, Special Publication 22, p. 190-204.

Crowell, J. C., Late Cenozoic basins of onshore southern California, 1987. Complexity is the hallmark of their tectonic history, in Cenozoic Basin Development of Coastal California, Rubey vol. 6, edited by R. V. Ingersoll and W. G. Ernst, pp. 207-241, Prentice- Hall, Englewood Cliffs, N.J.

Dai, F.C., C.F. Lee, J.H. Deng, L.G. Tham, 2005, The 1786 earthquake-triggered landslide dam and subsequent dam-break flood on the Dadu River, southwestern China, Geomorphology, vol. 65, no. 3-4, p. 205-221.

DeCelles, P.G. and K.A. Giles, 1996, Foreland Basin Systems, Basin Research, vol. 8, p. 105-123.

DeLong, S.B. & L.J. Arnold, 2006, Dating alluvial deposits with optically stimulated luminescence, AMS 14C and cosmogenic techniques, western Transverse Ranges, California, USA, Quaternary Geochronology, vol. 2, no. 1-4, p. 129-136.

DeVecchio, D.E., R.V. Heermance, M. Fuchs, & L.A. Owen, in press, Climate-controlled landscape evolution in the Western Transverse Ranges, California: Insights from Quaternary geochronology of the Saugus Formation and strath terrace flights, Lithosphere.

DeVecchio, D., 2009, Late Pleistocene to Holocene geomorphic and structural evolution of the Camarillo Fold Belt, California, University of California Santa Barbara Ph.D. dissertation, 135 pgs.

Dibblee, T.W., 1987a, Geologic Map of the Ojai Quadrangle, Ventura County, California; U.S. Geological Survey Open-File Report 82-72; map scale 1:24,000.

Dibblee, T.W., 1987b, Geologic Map of the Matilija Quadrangle, Ventura County, California; U.S. Geological Survey Open-File Report 82-72; map scale 1:24,000.

Dibblee, T.W., 1990, Geologic Map of the Santa Paula Peak Quadrangle, Ventura County, California; U.S. Geological Survey Open-File Report 82-72; map scale 1:24,000.

Donnellan, A., Hager, B.H., and King, R.W., 1993. Discrepancy between geological and geodetic deformation rates in the Ventura basin, Nature, v. 366, p. 333-336.

Fillion, L., F. Quinty, & C. Begin, 1991, A chronology of landslide activity in the valley of Riviere du Gouffre, Charlevoix, Quebec, Canadian Journal of Earth Sciences, vol. 28, no. 2, p. 250-256.

Fouch, T.D. and W.E. Dean, 1982, Lacustrine and Associated Clastic Depositional Environments; pp. 87-114 *in* Scholle, P.A. and Spearing, D., eds., Sandstone Depositional Environments; AAPG Memoir 31; 410 p.

Granger, D.E., and Muzikar, P.F., 2001, Dating sediment burial with in situ-produced cosmogenic nuclides: theory, techniques, and limitations, Earth And Planetary Science Letters, v. 188, p. 269-281.

Granger, D.E., D. Fabel, and A.N. Palmer, 2001, Pliocene–Pleistocene incision of the Green River, Kentucky, determined from radioactive decay of cosmogenic 26Al and 10Be in Mammoth Cave sediments, Geol. Soc. Am. Bulletin, vol. 113 p. 825–836.

Granger, D.E., and Smith, A.L., 2000, Dating buried sediments using radioactive decay and muogenic production of Al-26 and Be-10, Nuclear Instruments & Methods In Physics Research Section B-Beam Interactions with Materials and Atoms, v. 172, p. 822-826.

Heermance, R.V., Chen, J., Burbank, D.W., and Wang, C., 2007, Chronology and tectonic controls of Late Tertiary deposition in the southwestern Tian Shan foreland, NW China. Basin Research, vol. 19, p. 599-632.

Howard, J.L., 2005, Conglomerates of the Upper Middle Eocene to Lower Miocene Sespe Formation along the Santa Ynez Fault—Implications for the Geologic History of the Eastern Santa Maria Basin Area, California, chapter H, U.S. Geological Survey Bulletin 2005, *ed.* Margaret A. Keller.

Holm, R.F., 2001, Cenozoic paleogeography of the central Mogollon Rim- southern Colorado Plateau region, Arizona, revealed by tertiary gravel deposits, Oligocene to Pleistocene lave flows, and incised stream, Geological Society of America Bulletin, vol. 113, p. 1467-1485.

Horton, B.K., Yin, A., Spurlin, M.S., Zhou, J., and Wang, J., 2002, Paleocene-Eocene syncontractional sedimentation in narrow lacustrine-dominated basins of east-central Tibet, GSA Bulletin, vol. 114, no. 7, p. 771-786.

Huftile, G.J., Yeats, R.S., 1995, Convergence rates across a displacement transfer zone in the western Transverse Ranges, Ventura basin, California. Journal of Geophysical Research, vol. 100, no. B2, pp. 2043-2067.

Huftile, G.J. and R.S. Yeats, 1996. Deformation Rates across Placerita (Northridge Mw = 6.7 Aftershock Zone) and Hopper Canyon Segments of the Western Transverse Ranges Deformation Belt: Bulletin of the Seismological Society of America, v. 86, n. 1B, p. S3-S18.

Jackson, J., Molnar, P., 1990, Active Faulting and Block Rotations in the western Transverse Ranges, California, Journal of Geophysical Research, vol. 95, no. B13, pgs. 22,073-22,087.

Kear, J., 2005, Hydrogeology of the Ojai Groundwater Basin: Storativity and Confinement, Ventura County, California, California State University Northridge Masters' Thesis, 179 p.

Kong, P., D.E. Granger, F.Y Wu, M.W. Caffee, Y.J. Wang, X.T. Zhao, and Y. Zheng, 2009, Cosmogenic nuclide burial ages and provenance of the Xigeda paleo-lake: Implications for evolution of the Middle Yangtze River, Earth and Planetary Science Letters, vol. 278, p. 131-141.

Korup, O., 2004, Geomorphic characteristics of New Zealand landslide dams, Engineering Geology, vol. 73, no. 1-2, p. 13-35.

Korup, O. & F. Tweed, 2007, Ice, moraine, and landslide dams in mountainous terrain, Quaternary Science Reviews, vol. 26, no. 25-28, p. 3406-3422.

Kumar, R., N. Suresh, S.J. Sangode, and V. Kumaravel, 2007, Evolution of the Quaternary alluvial fan system in the Himalayan foreland basin: Implications for tectonic and climatic decoupling, Quaternary International, vol. 159, p. 6-20.

Lagoe, M.B., and P.R. Thompson, 1988, Chronostratigraphic significance of late Cenozoic planktonic foraminifera from the Ventura basin, California: Potential for improving tectonic and depositional interpretation, Journal of Foraminiferal Research, v. 18, p. 250-266.

Lal, D., 1991, Cosmic-ray labeling of erosion surfaces, in - situ nuclide production-rates and erosion models, Earth And Planetary Science Letters, v. 104, p. 424-439.

Lajoie, K.R., A.M. Sarna-Wojcicki, and R.F. Yerkes, 1982, Quaternary chronology and rates of crustal deformation in the Ventura area, California: GSA Cordilleran Section Field Trip Guidebook, p. 43-51.

Levi, S., and R. S. Yeats, 1993, Paleomagnetic constraints on the initiation of uplift on the Santa Susana fault, western Transverse Ranges, California, Tectonics, 12, 688-702.

Link, M.H. and R.H Osborne, 1978, Lacustrine facies in the Pliocene Ridge Basin Group: Ridge Basin, California *in* Albert Matter, and M.E. Tucker, eds., Modern and

ancient lake sediments: International Assoc. Sedimentologists, Spec. Pub. No. 2, p. 169-187.

Lisiecki, L.E. & M.E. Raymo, 2007, Plio-Pleistocene climate evolution: trends and transitions in glacial cycle dynamics, Quaternary Science Reviews, vol. 26, p. 56-69.

Luyendyk, B. P., M. J. Kamerling, R. R. Terres. And J. S. Hornafius, 1985, Simple shear of southern California during Neogene time suggested by paleomagnetic declinations, Journal of Geophysical Research, 90, 12,454-12,466.

Luyendyk, B.P., 1991, A model for Neogene crustal rotations, transtension, and transpression in southern California: Geological Society of America Bulletin, v. 103, p. 1528-1536.

Madden, C.L., C.M. Rubin, and A. Streig, 2006, Holocene and Latest Pleistocene Activity on the Mesquite Lake Fault near Twentynine Palms, Eastern California Shear Zone: Implications for Fault Interaction, Bulletin of the Seismological Society of America, vol. 96, p. 1305-1320.

Matmon, A., Y, Enzel, E. Zilberman, & A. Heimann, 1999, Late Pliocene and Pleistocene reversal of drainage systems in northern Israel: tectonic implications, Geomorphology, vol. 28, p. 43-59.

McLane, M., 1995, Sedimentology; Oxford University Press, Oxford; 423 p.

Mudelsee, M & M. Schulz, 1997, The Mid-Pleistocene climate transition: onset of 100 ka cycle lags ice volume build-up by 280 ka, Earth and Planetary Science Letters, vol. 151, p. 117-123.

Middleton, G.V. & M.A. Hampton, 1976, Sub-aqueous sediment transport and deposition by sediment gravity flows, *in* Stanley, D.H. & D.J.P. Swift, (eds.), Marine sediment transport and environmental management: John Wiley & Sons, Inc., Fig. 9, p. 213.

Nicholson, C., M.J. Kamerling, C.C. Sorlien, T.E. Hopps, and J.P. Gratier, 2007, Subsidence, Compaction, and Gravity Sliding: Implications for 3D Geometry, Dynamic Rupture, and Seismic Hazard of Active Basin-Bounding Faults in Southern California, Bulletin of the Seismological Society of America, Vol. 97, no. 5, pp. 1607-1620.

Nilsen, T.H., 1982, Alluvial fan deposits; pp. 49-86 *in* Scholle, P.A. and Spearing, D., eds., Sandstone Depositional Environments; AAPG Memoir 31; 410 p.

Nishiizumi, K., M.C. Imamura, M.W. Caffee, J.R. Southon, R.C. Finkel, and J. McAninch, 2007, Absolute calibration of ^{10}Be AMS standards, Nuclear Instruments and Methods in Physics Research Section B: Beam Interactions with Materials and Atoms, v. 258, p. 403.

Norris, T.L., Gancarz, A.J., Rokop, D.J., and Thomas, K.W., 1983, Half-life of 26Al: Proceedings of the Fourteenth Lunar and Planetary Science Conference, Part: Journal of Geophysical Research, v. 88, p. B331-B333.

Ori, G., Friend, P., 1984, Sedimentary basins, formed and carried piggy-back on active thrust sheets, Geology, vol. 12, p. 475-478.

Plint, A.G. & G.H. Browne, 1994, Tectonic event stratigraphy in a fluvio-lacustrine, strike-slip setting: the Boss Point Formation (Westphalian A), Cumberland Basin, Maritime Canada. J. Sed. Res., vol. B 64, p. 341–364.

Pratt-Sitaula, B., M. Garde, D.W. Burbank, M. Oskin, A. Heimsath, & E. Gabet, 2007, Bedload-to-suspended load ratio and rapid bedrock incision for Himalayan landslide-dam lake record, Quaternary Research, vol. 68, no. 1, p. 111-120.

Reimer, P. J., Baillie, M. G. L., Bard, E., Bayliss, A., Beck, J. W., Blackwell, P. G., Bronk Ramsey, C., Buck, C. E., Burr, G. S., Edwards, R. L., Friedrich, M., Grootes, P. M., Guilderson, T. P., Hajdas, I., Heaton, T. J., Hogg, A. G., Hughen, K. A., Kaiser, K. F., Kromer, B., McCormac, F. G., Manning, S. W., Reimer, R. W., Richards, D. A., Southon, J. R., Talamo, S., Turney, C. S. M., van der Plicht, J., & Weyhenmeyer, C. E., 2009, IntCal09 and Marine09 radiocarbon age calibration curves, 0-50,000 years cal BP, Radiocarbon, vol. 51, no. 4, p.1111-1150.

Rockwell, T.K., 1983, Soil chronology, geology, and neotectonics of the north central Ventura basin, California, University of California Santa Barbara Ph. D. dissertation, 424 pp.

Rockwell, T.K., E.A. Keller, M.N. Clark, and D.L. Johnson, 1984, Chronology and rates of faulting of Ventura River terraces, California, GSA Bulletin, v. 95, p. 1466-1474.

Rockwell, T.K., 1988, Neotectonics of the San Cayetano Fault, Transverse Ranges, California, GSA Bulletin, v. 100, p. 500-513.

Sarna-Wojcicki, A.M., H.R. Bowman, C.E. Meyer, P.C. Russell, M.J. Woodward, G. McCoy, J.J. Rowe, Jr., P.A. Baedecker, F. Asaro, and H. Michael, 1984, Chemical analyses, correlations, and ages of the upper Pliocene and Pleistocene ash layers of east-central and southern California: USGS Professional Paper 1293, 38 p.

Searle, M.P., K.T. Pickering, and D.J.W. Cooper, 1990, Restoration and evolution of the intermontane Indus molasses basin, Ladakh Himalaya, India, Tectonophysics, vol. 174, n. 3-4, p. 301-314.

Stock, G.M., R.S. Anderson, and R.C. Finkel, 2004, Pace of landscape evolution in the Sierra Nevada, California, revealed by cosmogenic dating of cave sediments, Geology, Vol. 32, p. 193-196.

Stuiver, M. & H.A. Polach, 1977, Discussion: Reporting of 14C Data, Radiocarbon, vol. 19, no. 3, p. 355-363.

Tan, S.S., P.J. Irvine, C.I. Gutierrez, 2005a, Geologic map of the Ojai 7.5' quadrangle, Ventura County, California: A digital database, version 1.0: California Department of Conservation California Geological Survey, scale 1:24,000.

Tan, S.S., P.J. Irvine, C.I. Gutierrez, 2005b, Geologic map of the Santa Paula Peak 7.5' quadrangle, Ventura County, California: A digital database, version 1.0: California Department of Conservation California Geological Survey, scale 1:24,000.

Tan, S.S., T.A. Jones, C.I. Gutierrez, 2006, Geologic map of the Matilija 7.5' quadrangle, Ventura County, California: A digital database, version 1.0: California Department of Conservation California Geological Survey, scale 1:24,000.

Trauth, M.H. & M.R. Strecker, 1999, Formation of landslide-dammed lakes during a wet period between 40,000 and 25,000 yr B.P. in northwestern Argentina, Palaeogeography, Palaeoclimatology, Palaeoecology, vol. 153, no. 1-4, p. 277-287.

Trauth, M.H., B. Bookhagen, N. Marwan, M.R. Strecker, 2003, Multiple landslide clusters record Quaternary climate changes in the northwestern Angentine Andes, Palaeogeography, Palaeoclimatology, Palaeoecology, vol. 194, no. 1-3, p. 109-121.

Villani, F. & S. Pierdominici, 2010, Late Quaternary tectonics of the Vallo di Diano basin (southern Apennines, Italy), Quaternary Science Reviews, vol. 29, p. 3167-3183.

Wehmiller, J. F., Lajoie, K. R., Sarna-Wojcicki, A. M., Yerkes, R. F., Kennedy, G. L., Stephens, T. A., and Kohl, R. F., 1978, Amino-acid racemization dating of Quaternary mollusks, Pacific Coast, United States, *in* Zartman, R. E., ed., 14th International Conference on Geochronology, Cosmochronology, Isotope Geology, Short Papers: U. S. Geological Survey Open-File Report 78-7001, p. 445-448.

Wehmiller, J.F., 1992, Aminostratigraphy of southern California Quaternary marine terraces, in Quaternary Coasts of the United States: Marine and Lacustrine Systems, Spec. Publ. 48, Soc. Econ. Paleontol. Mineral., p. 317-321.

Yeats, R.S., Clark, M.N., Keller, E.A., and Rockwell, T.K., 1981. Active fault hazard in southern California: Ground rupture versus seismic shaking, GSA Bulletin, Part 1, v. 92, p. 198-196.

Yeats, R.S., 1981, Quaternary flake tectonics of the California Transverse Ranges, Geology, vol. 9, no. 1, p. 16-20.

Zachos, J., M. Pagani, L. Sloan, E. Thomas, & K. Billups, 2001, Trends, rhythms, and aberrations in global climate 65 Ma to the present, Science, vol. 292, p. 386–392.